HAL
open science

Complete systems of inequalities relating the perimeter, the area and the Cheeger constant of planar domains

Ilias Ftouhi

To cite this version:

Ilias Ftouhi. Complete systems of inequalities relating the perimeter, the area and the Cheeger constant of planar domains. 2022. hal-03006019v6

HAL Id: hal-03006019

https://hal.science/hal-03006019v6

Preprint submitted on 17 Jul 2022

HAL is a multi-disciplinary open access archive for the deposit and dissemination of scientific research documents, whether they are published or not. The documents may come from teaching and research institutions in France or abroad, or from public or private research centers.

L'archive ouverte pluridisciplinaire **HAL**, est destinée au dépôt et à la diffusion de documents scientifiques de niveau recherche, publiés ou non, émanant des établissements d'enseignement et de recherche français ou étrangers, des laboratoires publics ou privés.

Complete systems of inequalities relating the perimeter, the area and the Cheeger constant of planar domains

Ilias Ftouhi

July 17, 2022

Abstract

The object of the paper is to find complete systems of inequalities relating the perimeter P, the area $|\cdot|$ and the Cheeger constant h of planar sets. To do so, we study the so called Blaschke–Santaló diagram of the triplet $(P, h, |\cdot|)$ for different classes of domains: simply connected sets, convex sets and convex polygons with at most N sides. We completely determine the diagram in the latter cases except for the class of convex N-gons when $N \geq 5$ is odd: therein, we show that the boundary of the diagram is given by the graphs of two continuous and strictly increasing functions. An explicit formula for the lower one and a numerical method to obtain the upper one is provided. At last, some applications of the results are presented.

Keywords: Cheeger constant, complete systems of inequalities, Blaschke–Santaló diagrams, convex sets.
AMS classification: 52A10, 52A40, 65K15.

1 Introduction and main results

Let Ω be a bounded subset of $\mathbb{R}^n$ (where $n \geq 2$). The Cheeger problem consists in studying the following minimization problem

$$h(\Omega) := \inf \left\{ \frac{P(E)}{|E|} \;\middle|\; E \text{ measurable and } E \subset \Omega \right\}, \tag{1}$$

where $P(E)$ is the distributional perimeter of E measured with respect to $\mathbb{R}^n$ (see for example [31] for definitions) and $|E|$ is the n-dimensional Lebesgue measure of E. The quantity $h(\Omega)$ is called *the Cheeger constant of* Ω and any set $C_\Omega \subset \Omega$ for which the infimum is attained is called a *Cheeger set of* Ω.

Since the early work of Jeff Cheeger [14], many authors took interest in the Cheeger problem has interested various authors. An introductory survey on the subject is referenced in [31]. We recall that every bounded domain Ω with Lipschitz boundary admits at least one Cheeger set C_Ω, see for example [31, Proposition 3.1]. In [1], the authors prove the uniqueness of the Cheeger set when $\Omega \subset \mathbb{R}^n$ is convex, but as far as we know there is no complete characterization of C_Ω in dimension $n \geq 3$ (even when convexity is assumed), in contrast to the planar case which was treated by Bernd Kawohl and Thomas Lachand-Robert in [26] where a complete description of the Cheeger sets of planar convex domains is given in addition to an algorithm to compute the Cheeger constant of convex polygons. We finally refer to [27, 28, 29] for recent results in larger classes of sets.

In this paper, we aim to describe all possible geometrical inequalities involving the perimeter, the area and the Cheeger constant of a given planar shape. It comes down to studying a so called Blaschke–Santaló diagram of the triplet $(P, h, |\cdot|)$.

Such a diagram allows to visualize all possible inequalities between three geometrical quantities. It is named after Blaschke and Santaló in reference to their works [4, 35], where they first introduced this notion. Afterward, these diagrams have been extensively studied, especially for the class of planar convex sets. We refer to [24] for more details and various examples involving geometrical functionals. We also refer to [9, 17, 18, 21, 30, 39, 40] for some recent results.

For more precision, let us define the Blaschke–Santaló diagrams we are interested in in this paper.

Definition 1. *Given $\mathcal{F}$ a class of measurable planar sets of, we define*

$$\begin{aligned} \mathcal{D}_{\mathcal{F}} &:= \Big\{ (x,y) \in \mathbb{R}^2,\ \exists\, \Omega \in \mathcal{F} \textit{ such that } |\Omega| = 1, P(\Omega) = x,\ h(\Omega) = y \Big\} \\ &:= \Big\{ \big(P(\Omega), h(\Omega)\big),\ \Omega \in \mathcal{F},\ |\Omega| = 1 \Big\}. \end{aligned}$$

We note that thanks to the following scaling properties:

$$\forall t > 0, \quad h(t\Omega) = \frac{h(\Omega)}{t}, \quad |t\Omega| = t^2|\Omega| \quad \text{and} \quad P(t\Omega) = tP(\Omega),$$

one can give a scale-invariant formulation of the diagram

$$\begin{aligned} \mathcal{D}_{\mathcal{F}} &= \left\{(x,y) \in \mathbb{R}^2, \ \exists \Omega \in \mathcal{F} \text{ such that } P(\Omega)/|\Omega|^{1/2} = x, \ |\Omega|^{1/2} h(\Omega) = y\right\} \\ &= \left\{ \left(\frac{P(\Omega)}{|\Omega|^{1/2}}, |\Omega|^{1/2} h(\Omega) \right), \ \Omega \in \mathcal{F} \right\}. \end{aligned}$$

In the whole paper, we denote by:

- $\mathcal{S}^2$ the set of bounded, planar and non-empty simply connected sets,
- $\mathcal{K}^2$ the set of bounded, planar and non-empty convex sets,
- $\mathcal{P}_N$ the set of convex polygons of at most N sides,
- B the disk of unit area,
- R_N a regular polygon of N sides and unit area,
- d^H the Hausdorff distance, see for example [22, Chapter 2] for the definition and more details,
- $d(\Omega)$ and $r(\Omega)$ respectively the diameter and inradius of the set Ω.

We are aiming at describing all possible inequalities relating P, $|\cdot|$ and h for different classes of planar sets and thus describing the associated Blaschke–Santaló diagrams. Let us first state the inequalities that we already know; if Ω is measurable, we have :

- the isoperimetric inequality:
$$\frac{P(\Omega)}{|\Omega|^{1/2}} \geq \frac{P(B)}{|B|^{1/2}} = 2\sqrt{\pi}, \tag{2}$$
- a consequence of the definition of the Cheeger constant
$$h(\Omega) = \inf_{E \subset \Omega} \frac{P(E)}{|E|} \leq \frac{P(\Omega)}{|\Omega|}, \tag{3}$$
- a Faber-Krahn type inequality:
$$|\Omega|^{1/2} h(\Omega) \geq |B|^{1/2} h(B) = \frac{P(B)}{|B|^{1/2}} = 2\sqrt{\pi}. \tag{4}$$

We note that each inequality may be visualized in the Blaschke–Santaló diagram as the hypograph or subgraph of a given function, see Figure 1 for example.

It is natural to wonder if there are other inequalities. Yet, the answer is tightly related to the choice of the class of sets $\mathcal{F}$. In the present paper, we are interested in studying complete systems of inequalities relating the perimeter P, the Cheeger constant h and the area $|\cdot|$ for three classes of planar sets:

1. The class of simply connected sets.
2. The class of convex sets.
3. The classes of convex polygons of at most N sides, where $N \geq 3$.

1.1 Results on the classes of simply connected and convex set

We provide the complete descriptions of the Blaschke–Santaló diagrams of the triplet $(P, h, |\cdot|)$ for both the classes $\mathcal{S}^2$ of planar simply connected sets and $\mathcal{K}^2$ of planar convex sets.

Theorem 2. *We take $x_0 = P(B) = 2\sqrt{\pi}$.*

1. *The diagram of the class $\mathcal{S}^2$ of planar simply connected domains is given by*

$$\mathcal{D}_{\mathcal{S}^2} = \{(x_0, x_0)\} \cup \{(x, y) \mid x > x_0 \text{ and } x_0 < y \leq x\}.$$

2. *The diagram of the class $\mathcal{K}^2$ of planar convex domains is given by*

$$\mathcal{D}_{\mathcal{K}^2} = \left\{(x, y) \;\middle|\; x \geq x_0 \text{ and } \frac{x}{2} + \sqrt{\pi} \leq y \leq x\right\}.$$

The study of the boundary of the Blaschke–Santaló diagram $\mathcal{D}_{\mathcal{K}^2}$ is a crucial step toward its complete description. Thus, we introduce the following definition of upper and lower boundaries:

Definition 3. *We take $x_0 = P(B) = 2\sqrt{\pi}$. We define the upper boundary of the diagram $\mathcal{D}_{\mathcal{K}^2}$ as follows:*

$$\{(x, y_x) \mid x \geq x_0\},$$

where

$$y_x := \sup\{h(\Omega) \mid \Omega \in \mathcal{K}^2,\ P(\Omega) = x \text{ and } |\Omega| = 1\} \in \mathbb{R},$$

and the lower boundary of the diagram $\mathcal{D}_{\mathcal{K}^2}$ as follows:

$$\{(x, y_x) \mid x \geq x_0\},$$

where

$$y_x := \inf\{h(\Omega) \mid \Omega \in \mathcal{K}^2,\ P(\Omega) = x \text{ and } |\Omega| = 1\} \in \mathbb{R}.$$

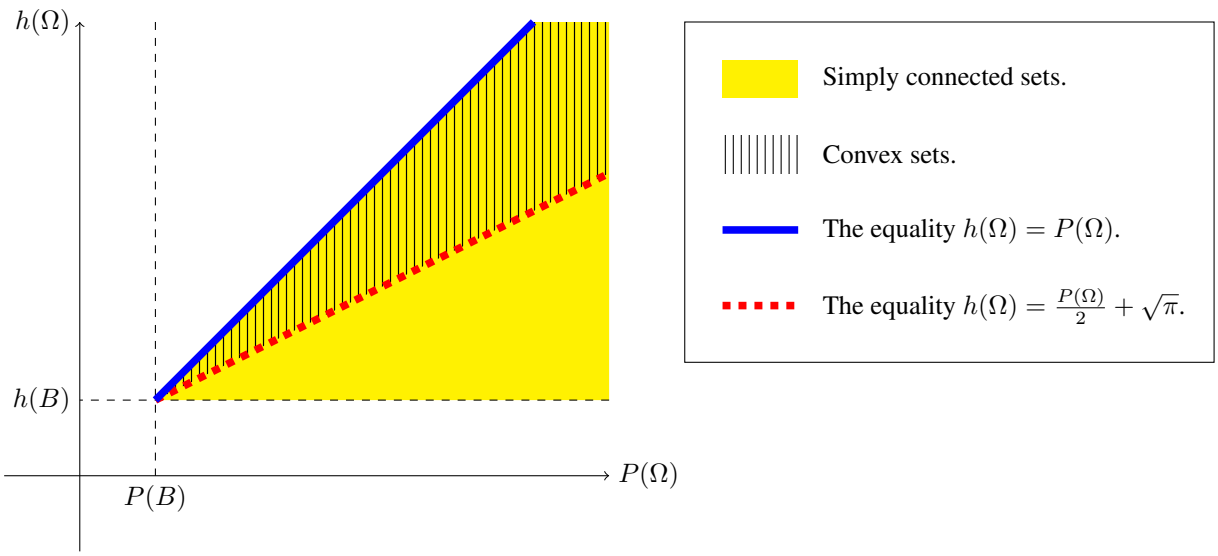

Figure 1: The Blaschke–Santaló diagrams for the classes of simply connected sets and convex sets.

We note that by taking advantage of the inequalities (2) and (4), it is also classical to represent the Blaschke–Santaló diagrams as subsets of $[0, 1]^2$. In our situation, this means to consider the sets

$$\mathcal{D}'_{\mathcal{F}} := \left\{(X, Y) \mid \exists \Omega \in \mathcal{F} \text{ such as } |\Omega| = 1 \text{ and } (X, Y) = \left(\frac{P(B)}{P(\Omega)}, \frac{h(B)}{h(\Omega)}\right)\right\} \subset [0, 1]^2,$$

where $\mathcal{F}$ is a given class of planar sets. With this parametrization, the Blaschke–Santaló diagrams for the classes $\mathcal{S}^2$ and $\mathcal{K}^2$ are given by the following sets:

$$\begin{cases} \mathcal{D}'_{\mathcal{S}^2} = \{(1, 1)\} \cup \{(X, Y) \mid X \in (0, 1) \text{ and } X \leq Y < 1\}, \\ \mathcal{D}'_{\mathcal{K}^2} = \{(X, Y) \mid X \in (0, 1] \text{ and } X \leq Y \leq \frac{2X}{1+X}\}, \end{cases}$$

which are represented in Figure 2.

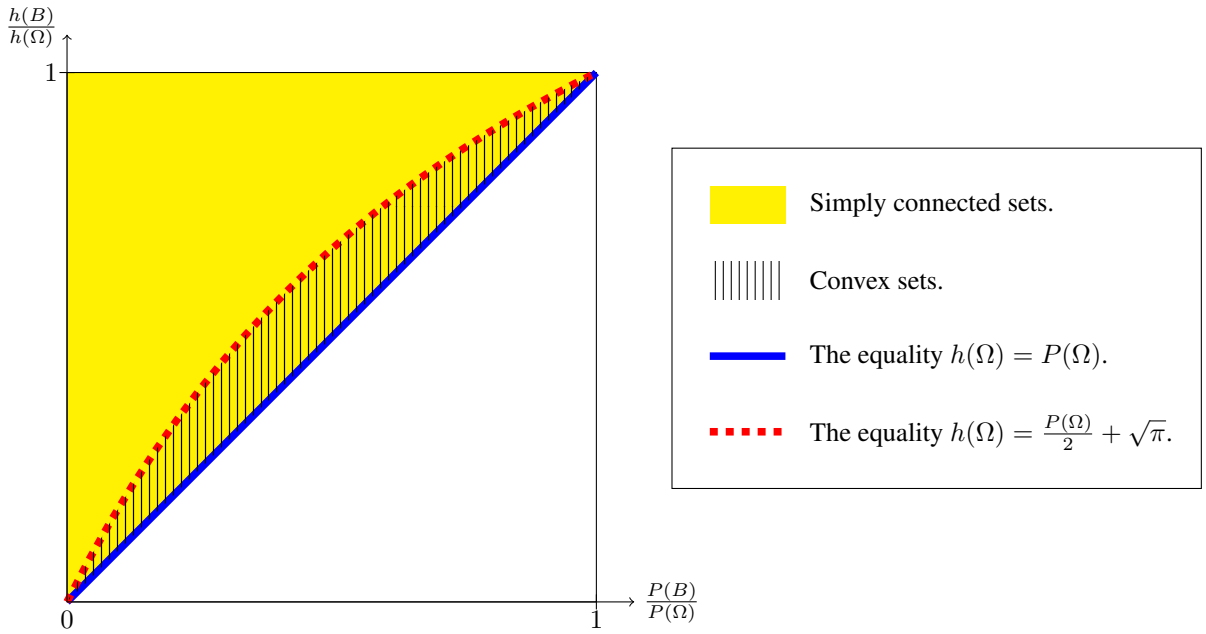

Figure 2: The Blaschke–Santaló diagrams for the classes of simply connected sets and convex sets represented in $[0,1]^2$.

Let us give some comments on the latter results:

- One major step in the study of the diagram of convex sets is to prove the following sharp inequality

$$\forall \Omega \in \mathcal{K}^2, \quad h(\Omega) \geq \frac{P(\Omega) + \sqrt{4\pi|\Omega|}}{2|\Omega|}, \tag{5}$$

  where equality occurs for example for circumscribed polygons (i.e., those whose sides touch their incircles) and more generally for sets which are homothetical to their form bodies[1].

- The inequality (5) is rather easy to prove when the convex Ω is a Cheeger-regular polygon (that is, its Cheeger set touches all of its sides), see [11, Remark 32], but much difficult to prove for general convex sets as shown in the present paper (see Section 3.1). We also note that this inequality may be seen as a quantitative isoperimetric inequality for the Cheeger constant of convex planar sets. Indeed, it can be written in the following form

$$\forall \Omega \in \mathcal{K}^2, \quad |\Omega|^{1/2} h(\Omega) - |B|^{1/2} h(B) \geq \frac{1}{2}\left(\frac{P(\Omega)}{|\Omega|^{1/2}} - \frac{P(B)}{|B|^{1/2}}\right) \geq 0.$$

  We refer to [19, 25] for some examples of quantitative inequalities for the Cheeger constant.

  Moreover, we note in Section 5.1 that the inequality (5) is stronger than a classical result [10, Theorem 3] due to R. Brooks and P. Waksman. It also improves in the planar case a more recent estimate given in [7, Corollary 5.2], which states that for any open, bounded and convex set $\Omega \subset \mathbb{R}^n$, where $n \geq 2$, one has

$$h(\Omega) \geq \frac{1}{n} \cdot \frac{P(\Omega)}{|\Omega|}.$$

- We note that the first statement of Theorem 2 asserts that the inequalities (3) and (4) form a complete system of inequalities of the triplet $(P, h, |\cdot|)$ in any class of planar sets that contains $\mathcal{S}^2$. Meanwhile, the second one asserts that this is no longer the case for the class $\mathcal{K}^2$ of planar and convex sets, where estimates (3) and (5) are shown to be forming a complete system of inequalities for the triplet $(P, h, |\cdot|)$.

- One could wonder why we chose to work with the class of simply connected sets. The main reason is that for any subclass of measurable domains that contains the simply connected ones, the diagram is the same. Indeed, if we denote by $\mathcal{C}^2$ a subclass of planar and measurable sets that contains the class $\mathcal{S}^2$, we have by the inequalities (3) and (4) (where the equality holds in (4) only for balls)

$$\mathcal{D}_{\mathcal{C}^2} \subset \{(x_0, x_0)\} \cup \{(x, y) \mid x > x_0 \text{ and } x_0 < y \leq x\} = \mathcal{D}_{\mathcal{S}^2}.$$

  Moreover, the inclusion $\mathcal{S}^2 \subset \mathcal{C}^2$ implies that $\mathcal{D}_{\mathcal{S}^2} \subset \mathcal{D}_{\mathcal{C}^2}$, which proves the equality.

[1] We refer to [36, Page 386] for the definition of form bodies.

- We finally note that due to technical convenience, we first show the second assertion (the case of convex sets) and then use it to prove the first one (the case of simply connected sets).

1.2 Results on the classes of convex polygons

Now, let us focus on the class of convex polygons. We give an improvement of the inequality (3) in the class $\mathcal{P}_N$ of convex polygons with at most N sides, where $N \geq 3$. We recall that since triangles are circumscribed polygons, one has

$$\forall \Omega \in \mathcal{P}_3, \quad h(\Omega) = \frac{P(\Omega) + \sqrt{4\pi|\Omega|}}{2|\Omega|}, \tag{6}$$

see the discussion below [26, Theorem 3].

As for the case $N \geq 4$, we prove the following sharp inequality

$$\forall \Omega \in \mathcal{P}_N, \qquad h(\Omega) \leq \frac{P(\Omega) + \sqrt{P(\Omega)^2 + 4\big(\pi - N\tan\frac{\pi}{N}\big)|\Omega|}}{2|\Omega|}, \tag{7}$$

with equality if and only if Ω is Cheeger-regular (i.e., all its sides touch its Cheeger set C_Ω) and all of its angles are equal (to $(N-2)\pi/N$). The equality is also asymptotically attained by the following family $\big([0,1]\times[0,d]\big)_{d\geq 1}$ of rectangles when d goes to infinity.

In order to simplify the notation, we denote by $\mathcal{D}_N := \mathcal{D}_{\mathcal{P}_N}$ the Blaschke–Santaló diagram of the triplet $(P, h, |\cdot|)$ for the class of convex polygons of at most N sides, see Definition 1 for the notion of Blaschke–Santaló diagrams.

As for the case of convex sets, we introduce the notion of upper and lower boundaries of the diagram $\mathcal{D}_N$.

Definition 4. *Let $N \geq 3$, we recall that R_N corresponds to a regular polygon of N sides and unit area. We define the upper boundary of the diagram $\mathcal{D}_N$ as follows:*

$$\{(x, g_N(x)) \mid x \geq P(R_N)\},$$

where

$$g_N : x \longmapsto \sup\{h(\Omega) \mid \Omega \in \mathcal{P}_N,\ P(\Omega) = x \text{ and } |\Omega| = 1\} \in \mathbb{R},$$

and the lower boundary of the diagram $\mathcal{D}_N$ as follows:

$$\{(x, y_x) \mid x \geq P(R_N)\},$$

where

$$y_x := \inf\{h(\Omega) \mid \Omega \in \mathcal{P}_N,\ P(\Omega) = x \text{ and } |\Omega| = 1\} \in \mathbb{R}.$$

Theorem 5. *Let $N \geq 3$. The diagram $\mathcal{D}_N := \mathcal{D}_{\mathcal{P}_N}$ contains its upper and lower boundaries. Moreover, the lower boundary is given by the half line*

$$\left\{\left(x, \frac{x}{2} + \sqrt{\pi}\right) \mid x \geq P(R_N)\right\},$$

and the upper boundary is given by the graph of the continuous and strictly increasing function g_N

$$\{(x, g_N(x)) \mid x \geq P(R_N)\}.$$

Moreover, we have the following cases:

- *if $N = 3$, we have*

$$\mathcal{D}_3 = \left\{\left(x, \frac{x}{2} + \sqrt{\pi}\right) \,\middle|\, x \geq P(R_3)\right\}.$$

- *If N is even, then*

$$\mathcal{D}_N = \left\{(x, y) \mid x \geq P(R_N) \text{ and } \frac{x}{2} + \sqrt{\pi} \leq y \leq g_N(x)\right\},$$

  and

$$\forall x \geq P(R_N), \quad g_N(x) = \frac{x + \sqrt{x^2 + 4(\pi - N\tan\frac{\pi}{N})}}{2}.$$

- *If $N \geq 5$ is odd, there exist $c_N \geq b_N > P(R_N)$ such that*

$$\forall x \in [P(R_N), b_N], \quad g_N(x) = \frac{x + \sqrt{x^2 + 4(\pi - N \tan \frac{\pi}{N})}}{2}$$

and

$$\forall x \in \big[c_N, +\infty\big), \quad g_N(x) < \frac{x + \sqrt{x^2 + 4(\pi - N \tan \frac{\pi}{N})}}{2}.$$

Moreover

$$g_N(x) \underset{x \to +\infty}{\sim} x.$$

Let us give some comments on the latter results:

- For every $N \geq 3$, we have the inclusion $\mathcal{D}_N \subset \mathcal{D}_{N+1}$ (because $\mathcal{P}_N \subset \mathcal{P}_{N+1}$). Moreover, we notice that the right hand side of the inequality (7) (monotonically) converges to the right hand side of the inequality (3). Thus, one can recover the diagram $\mathcal{D}_{\mathcal{K}^2}$ of convex sets as the limit of $\mathcal{D}_N$. In fact, one can show that

$$\mathcal{D}_{\mathcal{K}^2} = \overline{\bigcup_{N=3}^{+\infty} \mathcal{D}_N},$$

  where $\overline{\bigcup_{N=3}^{+\infty} \mathcal{D}_N}$ corresponds to the closure of $\bigcup_{N=3}^{+\infty} \mathcal{D}_N$.

- It is interesting to note that Theorem 5 shows that the inequalities (5) and (7) form a complete system of inequalities of the triplet $(P, h, |\cdot|)$ in the class $\mathcal{P}_N$ if and only if N is even.

- We believe that $c_N = b_N$ for every N odd and greater or equal than 5. To prove it, one could be tempted to solve the shape optimization problems

$$\max\{h(\Omega) \mid |\Omega| = 1,\ P(\Omega) = p_0 \text{ and } \Omega \in \mathcal{P}_N\},$$

  where $p_0 \in [P(R_N), +\infty)$. Unfortunately, this seems to be quite challenging in this case, since numerical simulations (see Section 4) suggest that the solutions are not unique and for large values of p_0 they are not necessarily Cheeger-regular (i.e., all its sides touch its Cheeger set C_Ω) and thus one does not have an explicit formula for their Cheeger constants, see Theorem 11 and Lemma 16. Another possible strategy to prove the equality $c_N = b_N$ could be to show that one can continuously deform any Cheeger-regular N-gon Ω whose angles are all equal into a regular N-gon while making sure to preserve these two properties throughout the process.

- We note that we are able to prove the following estimate

$$c_N \leq 2N \sqrt{\tan \frac{(N-2)\pi}{2N}},$$

  see (26).

The present paper is organized as follows: Section 2 contains two subsections, in the first one we recall some classical definitions and results needed for the proofs, in the second one we state and prove some preliminary lemmas which are also interesting on their own. The proofs of the main theorems are given in Section 3. Then, we provide some numerical simulations on the diagrams $\mathcal{D}_N$ in Section 4. Finally, we give some applications of the results of our results in Section 5.

2 Classical results and preliminaries

2.1 Classical definitions and results

In this subsection, we recall some classical definitions and results that are used in the paper.

Theorem 6. *[16, Theorem 2 and Remark 3]*
Take $N \geq 3$ and $\Omega \subset \mathbb{R}^2$ a convex polygon of N sides. We define:

$$T(\Omega) := \sum_{i=1}^{N} \frac{1}{\tan \frac{\alpha_i}{2}}, \tag{8}$$

where $\alpha_i \in (0,\pi]$ are the interior angles of Ω. We have the following estimates:

$$N \tan \frac{\pi}{N} \leq T(\Omega) \leq \frac{P(\Omega)^2}{4|\Omega|}. \tag{9}$$

The lower bound is attained if and only if all the angles α_i are equal (to $\frac{N-2}{2N}\pi$), meanwhile the upper one is an equality if and only the polygon Ω is circumscribed.

Remark 7. *The lower bound is a simple application of Jensen's inequality to the function* cotan *which is strictly convex on $(0,\pi/2)$. On the other hand, since $N \tan \frac{\pi}{N} > \pi$, the upper estimate may be seen as an improvement of the isoperimetric inequality for convex polygons. We refer for example to [16] for a detailed proof of Theorem 6.*

Definition 8. *Let A and B be two subsets of $\mathbb{R}^2$ and $t > 0$, we define*

- *the Minkowski sum of the sets A and B by*

$$A \oplus B := \{x + y \mid x \in A \text{ and } y \in B\},$$

- *and the dilatation of the set A by the positive coefficient t by*

$$tA := \{tx \mid x \in A\}.$$

Definition 9. *For a given planar set Ω and any $x \in \Omega$, we denote by dist$(x, \partial\Omega)$ the distance from x to the boundary of Ω, and for $t \geq 0$, we denote by Ω_{-t} the sets of points of Ω of distance at least t to the boundary, i.e.,*

$$\Omega_{-t} := \{x \in \Omega \mid \text{dist}(x, \partial\Omega) \geq t\}.$$

The sets $(\Omega_{-t})_{t\geq 0}$ are known as the inner parallel sets of Ω.

Let us now recall some classical and important results on the Cheeger problem for planar convex sets.

Theorem 10. *[26, Theorem 1] Let Ω be a planar convex set. There exists a unique value $t = t^* > 0$ such that $|\Omega_{-t}| = \pi t^2$. We also have $h(\Omega) = 1/t^*$. Moreover, the Cheeger set of Ω is given by*

$$C_\Omega = \Omega_{-t^*} \oplus t^* B_1,$$

where B_1 is the unit disk.

Theorem 11. *[26, Theorem 3] If Ω is a Cheeger-regular polygon (i.e., all its sides touch its Cheeger set C_Ω), then,*

$$h(\Omega) = \frac{P(\Omega) + \sqrt{P(\Omega)^2 - 4\big(T(\Omega) - \pi\big)|\Omega|}}{2|\Omega|}, \tag{10}$$

where $T(\Omega)$ is defined in (8).

It is natural to wonder if the equality (10) holds for general convex polygons. In Lemma 16, we prove that there is only an inequality and that the equality occurs if and only if the polygon is Cheeger-regular.

Let us now recall some classical parametrizations of starshaped sets (or convex ones in particular). We refer to [36, Section 1.7] for more details.

Definition 12. *A set $\Omega \subset \mathbb{R}^2$ is called starshaped with respect to a point $A \in \mathbb{R}^2$, if it is not empty and for every $M \in \Omega$, the segment $[AM]$ is included in Ω.*

Let us now recall some important functions that allow to parametrize a given set Ω. If $\Omega \subset \mathbb{R}^2$ is a compact and starshaped with respect to the origin 0, we recall that

- its radial function is given by $f_\Omega : x \in \mathbb{R}^2\backslash\{0\} \longmapsto f_\Omega(x) = \max\{\lambda \geq 0 \mid \lambda x \in \Omega\}$,
- and its gauge function is given by $u_\Omega : \mathbb{R}^2\backslash\{0\} \longmapsto \inf\{\lambda \geq 0 \mid x \in \lambda\Omega\}$.

If Ω is convex (not necessarily containing the origin), its support function is defined as follows:

$$h_\Omega : x \in \mathbb{R}^2 \longmapsto \sup\{\langle x, y\rangle \mid y \in \Omega\}.$$

Since the functions f_Ω, u_Ω and h_Ω satisfy the following scaling properties $f_\Omega(tx) = tf_\Omega(x)$, $u_\Omega(tx) = t^{-1}u_\Omega(x)$ and $h_\Omega(tx) = th_\Omega(x)$ for $t > 0$, they can be characterized by their values on the unit sphere $\mathbb{S}^1$ or equivalently on the interval $[0, 2\pi)$.

In the present paper, the radial, gauge and support functions are defined on the interval $[0, 2\pi)$ as stated in the following definition.

Definition 13. *If $\Omega \subset \mathbb{R}^2$ is a compact and starshaped with respect to the origin 0,*

- *the radial function of Ω is given by $f_\Omega : \theta \in [0, 2\pi) \longmapsto \max\{\lambda \geq 0 \mid \lambda\binom{\cos\theta}{\sin\theta} \in \Omega\}$,*
- *the gauge function of Ω is given by $u_\Omega : [0, 2\pi) \longmapsto \inf\{\lambda \geq 0 \mid \binom{\cos\theta}{\sin\theta} \in \lambda\Omega\}$.*

If Ω is convex (not necessarily containing the origin), its support function is given by

$$h_\Omega : [0, 2\pi) \longmapsto \sup\left\{\left\langle \begin{pmatrix}\cos\theta \\ \sin\theta\end{pmatrix}, y\right\rangle \mid y \in \Omega\right\}.$$

Let us now give some important remarks on these functions.

Remark 14.
- *The functions introduced above can be defined in higher dimensions. We refer for example to [36, Section 1.7] for more details and results.*
- *The gauge function is the inverse of the radial function. Indeed, for every $\theta \in [0, 2\pi)$, we have $u_\Omega(\theta) = 1/f_\Omega(\theta)$.*
- *It is interesting to note that the gauge and support functions allow to provide a simple characterization of the convexity of a set Ω. Indeed, Ω is convex if and only if $h''_\Omega + h_\Omega \geq 0$, which is also equivalent to $u''_\Omega + u_\Omega \geq 0$.*
- *The support function has some nice properties:*
  - *it is linear for the Minkowski sum and dilatation. Indeed, if Ω_1 and Ω_2 are two convex bodies and $\alpha, \beta > 0$, we have*
  $$h_{\alpha\Omega_1+\beta\Omega_2} = \alpha h_{\Omega_1} + \beta h_{\Omega_2},$$
  see [36, Section 1.7.1].
  - *It also provides elegant formulas for some geometrical quantities. Fro example the perimeter of a convex body Ω is given by*
  $$P(\Omega) = \int_0^{2\pi} h_\Omega(\theta)d\theta,$$
  and the Hausdorff distance between two convex bodies Ω_1 and Ω_2 is given by
  $$d^H(\Omega_1, \Omega_2) = \sup_{\theta\in[0,2\pi)} |h_{\Omega_1}(\theta) - h_{\Omega_2}(\theta)|,$$
  see [36, Lemma 1.8.14].

At last, let us recall a classical result on the area of Minkowski sums. For more details and general results, we refer to [36].

Theorem 15. *There exist 3 bilinear (for Minkowski sum and dilatation) forms $W_k : \mathcal{K}^2 \times \mathcal{K}^2 \longrightarrow \mathbb{R}$, for $k \in [\![0; 2]\!]$, named Minkowski mixed volumes, such that for every $K_1, K_2 \in \mathcal{K}^2$ and $t_1, t_2 > 0$, we have*

$$|t_1K_1 + t_2K_2| = t_1^2W_0(K_1, K_2) + 2t_1t_2W_1(K_1, K_2) + t_2^2W_2(K_1, K_2). \tag{11}$$

Moreover, the W_k are continuous with respect to the Hausdorff distance, in the sense that if two sequences of convex bodies $(K_1^n)_n$ and $(K_2^n)_n$ respectively converge to some convex bodies K_1 and K_2 both with respect to the Hausdorff distance, one has

$$\lim_{n\to+\infty} W_k(K_1^n, K_2^n) = W_k(K_1, K_2).$$

2.2 Preliminary lemmas

In this section we prove some important Lemmas that we use in Section 3 for the proofs of the main results.

The following lemma[2] shows that the equality of Theorem 11 which is valid for Cheeger-regular polygons becomes an inequality for general polygons. Thus, we obtain an upper bound for the Cheeger constant of polygons that we use to prove the inequality (7).

[2]We are indebted to Jimmy Lamboley for the idea of proof of this lemma.

Lemma 16. *If Ω is a convex polygon, one has*

$$h(\Omega) \leq \frac{P(\Omega) + \sqrt{P(\Omega)^2 - 4\big(T(\Omega) - \pi\big)|\Omega|}}{2|\Omega|},$$

where $T(\Omega)$ is defined in (8)*. The equality occurs if and only if the polygon Ω is Cheeger-regular (i.e., all its sides touch its Cheeger set C_Ω).*

Proof. The number of sides of the inner sets $(\Omega_{-t})_t$ of a polygon (we refer to Definition 9 for the notion of inner sets) is decreasing with respect to $t \geq 0$. Actually, the function $t \in [0, r(\Omega)] \longmapsto n(t)$ (where $r(\Omega)$ is the inradius of Ω and $n(t)$ is the number of sides of Ω_{-t}) is a piece-wise constant decreasing function. We introduce the sequence $0 = t_0 < t_1 < \cdots < t_{N_\Omega} = r(\Omega)$, where $N_\Omega \in \mathbb{N}^*$, such that

$$\forall k \in [\![0, N_\Omega - 1]\!], \forall t \in [t_k, t_{k+1}), \qquad n(t) = n_k,$$

where $(n_k)_{k \in [\![0, N_\Omega - 1]\!]}$ is strictly decreasing.

In the computations below, we use the classical Steiner formulas (see [37]) for the perimeter and the area of inner (polygonal) sets. We have for every $k \in [\![1, N_\Omega]\!]$,

$$P(\Omega_{-t_k}) = P((\Omega_{-t_{k-1}})_{-(t_k - t_{k-1})}) = P(\Omega_{-t_{k-1}}) - 2(t_k - t_{k-1})T(\Omega_{-t_{k-1}}) \tag{12}$$

and

$$|\Omega_{-t_k}| = |(\Omega_{-t_{k-1}})_{-(t_k - t_{k-1})}| = |\Omega_{-t_{k-1}}| - (t_k - t_{k-1})P(\Omega_{-t_{k-1}}) + (t_k - t_{k-1})^2 T(\Omega_{-t_{k-1}}). \tag{13}$$

Let us take $t \in [0, r(\Omega)]$ and $k \in [\![1, N_\Omega]\!]$. We have

$$\begin{aligned}
|\Omega_{-t_k}| - (t - t_k)P(\Omega_{-t_k}) + (t - t_k)^2 T(\Omega_{-t_k}) &= |\Omega_{-t_{k-1}}| - (t_k - t_{k-1})P(\Omega_{-t_{k-1}}) + (t_k - t_{k-1})^2 T(\Omega_{-t_{k-1}}) \\
&\quad - (t - t_k)\big(P(\Omega_{-t_{k-1}}) - 2(t_k - t_{k-1})T(\Omega_{-t_{k-1}})\big) + (t - t_k)^2 T(\Omega_{-t_k}) \\
&> |\Omega_{-t_{k-1}}| - (t - t_{k-1})P(\Omega_{-t_{k-1}}) + (t - t_{k-1})^2 T(\Omega_{-t_{k-1}}),
\end{aligned}$$

where we used (12) and (13) for the equality and the fact that $T(\Omega_{-t_{k-1}}) < T(\Omega_{-t_k})$ for the inequality (see the equation (14) of [26]). By straightforward induction, we show that one has for every $k \in [\![1, N_\Omega]\!]$,

$$\forall t \in [0, r(\Omega)], \qquad |\Omega_{-t_k}| - (t - t_k)P(\Omega_{-t_k}) + (t - t_k)^2 T(\Omega_{-t_k}) \geq |\Omega| - tP(\Omega) + t^2 T(\Omega). \tag{14}$$

Now, let us take $k \in [\![0, N_\Omega - 1]\!]$ and $t \in [t_k, t_{k+1})$. We have the inequality

$$\begin{aligned}
g(t) := |\Omega_{-t}| - \pi t^2 = |(\Omega_{-t_k})_{-(t - t_k)}| - \pi t^2 &= |\Omega_{-t_k}| - (t - t_k)P(\Omega_{-t_k}) + (t - t_k)^2 T(\Omega_{-t_k}) - \pi t^2 \\
&\geq |\Omega| - tP(\Omega) + t^2 T(\Omega) - \pi t^2 =: f(t),
\end{aligned}$$

where the equality $g(t) = f(t)$ holds only on $[0, t_1]$. This inequality yields that $1/h(\Omega)$ which is the unique zero of g on $[0, r(\Omega)]$ (by Theorem 10), is larger than

$$\frac{2|\Omega|}{P(\Omega) + \sqrt{P(\Omega)^2 - 4\big(T(\Omega) - \pi\big)|\Omega|}},$$

the smallest zero of f,[3] with equality if and only if the zero of g is in $[0, t_1]$, which is the case if and only if the polygon Ω is Cheeger-regular (see [26, Theorem 3]). This ends the proof. □

Remark 17. *One interesting takeaway idea of proof of Lemma 16 is that since the Cheeger constant of a planar convex set is characterized via the area of inner sets (see Definition 9 and Theorem 10), one can use the estimates on the area of inner sets to obtain bounds on the Cheeger constant. This strategy is used in [20] to prove the following sharp inequality*

$$\forall \Omega \in \mathcal{K}^2, \quad h(\Omega) \leq \frac{1}{r(\Omega)} + \sqrt{\frac{\pi}{|\Omega|}},$$

where $r(\Omega)$ is the inradius of Ω.

[3] The second order polynomial function f admits two positive zeros. Since, f is continuous and $f(0) = |\Omega| > 0$ and $f(r(\Omega)) \leq g(r(\Omega)) = |\Omega_{-r(\Omega)}| - \pi r(\Omega)^2 = -\pi r(\Omega)^2 < 0$, we have by the Intermediate Value Theorem that the smallest zero of f is in the interval $(0, r(\Omega))$.

Since the inequality (5) is quite easy to obtain for Cheeger-regular polygons (because in this case we have an explicit formula for the Cheeger constant in terms of the perimeter, the area and the interior angles), it is natural when dealing with general polygons to try to come back to the case of Cheeger-regular ones. The following Lemma shows how to deform a given polygon into a Cheeger-regular one while preserving its Cheeger constant, increasing its perimeter and decreasing its area. This allows (as shown in **Step 2** of Section 3.1) to prove the inequality (5) for the case of general polygons.

Lemma 18. *Let Ω be a polygon. There exists a Cheeger-regular polygon $\widetilde{\Omega}$ such that: $|\Omega| \geq |\widetilde{\Omega}|$, $P(\Omega) \leq P(\widetilde{\Omega})$ and $h(\Omega) = h(\widetilde{\Omega})$.*

Proof. If Ω is Cheeger-regular, we take $\widetilde{\Omega} = \Omega$. Let us assume that the polygon Ω is not Cheeger-regular. We provide an algorithm to deform Ω into a Cheeger-regular polygon with the same Cheeger set (thus, also the same Cheeger value), larger perimeter and smaller area.

Since the polygon Ω is not Cheeger-regular, there exist three consecutive vertices, that we denote by X, Y and Z, such that at least one (or may be both) of the sides $[XY]$ and $[YZ]$ does not touch the Cheeger set C_Ω.

First step: using parallel chord movements

We begin by the case where both the sides $[XY]$ and $[YZ]$ do not touch C_Ω. We use a parallel chord movement. More precisely, we move Y along the line passing through Y and being parallel to the line (XZ). This way, the area is preserved, and the perimeter must increase when moving Y away from the perpendicular bisector of the side $[XZ]$ (which is possible at least in one direction). We assume without loss of generality that the direction which increases the perimeter is from Z to X (see Figure 3). We then move Y until one the following cases occurs:

1. the line (XY) becomes colinear to the other side of extremity X.
2. The side $[YZ]$ touches the boundary of C_Ω.

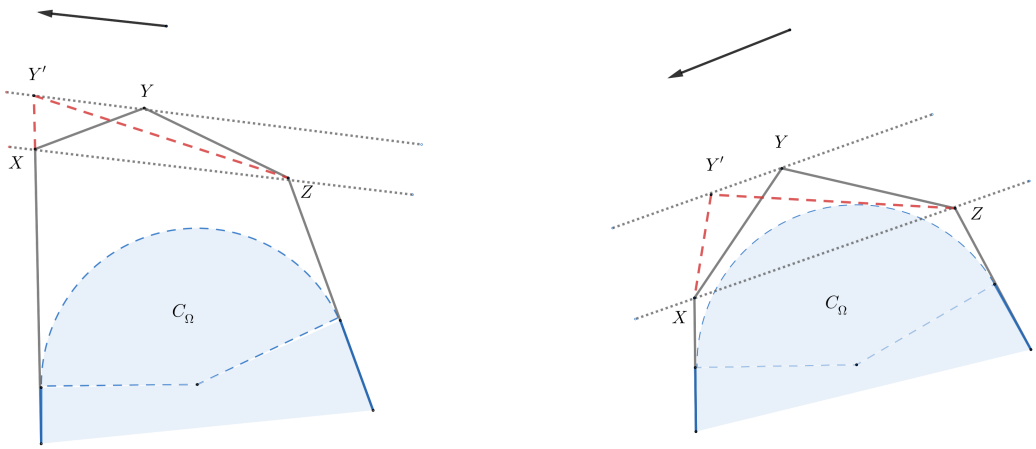

Figure 3: Case 1 on the left and case 2 on the right.

In both cases, the number of sides that do not touch ∂C_Ω decreases by one, while the area and the Cheeger constant are preserved and the perimeter is increased.

We iterate this process for all the vertices which are extremities of two sides that do not touch ∂C_Ω. Since the number of vertices is finite, in a finite number of steps, we obtain a polygon where there are no consecutive sides that do not touch ∂C_Ω.

Second step: rotating the remaining sides[4]

The second step is to "rotate" the remaining sides that do not touch ∂C_Ω in such a way to make them touch it (see Figure 4), in order to get a Cheeger-regular polygon with the same Cheeger constant, larger perimeter and smaller area. This kind of deformations is inspired by the work of D. Bucur and I. Fragalà [11].

We denote by

- α_1,$\alpha_2 \in (0, \pi)$ the interior angles of the polygon Ω respectively associated to the vertices X and Y,
- O the mid-point of the side $[XY]$,
- t the angle of our "rotation",
- X_t and Y_t the vertices of the new polygon denoted by Ω_t, obtained by rotating the side $[XY]$ around the mid-point O with the angle t.

The polygon Ω_t has the same vertices as Ω except X and Y that have respectively been mapped as X_t and Y_t, see Figure 4.

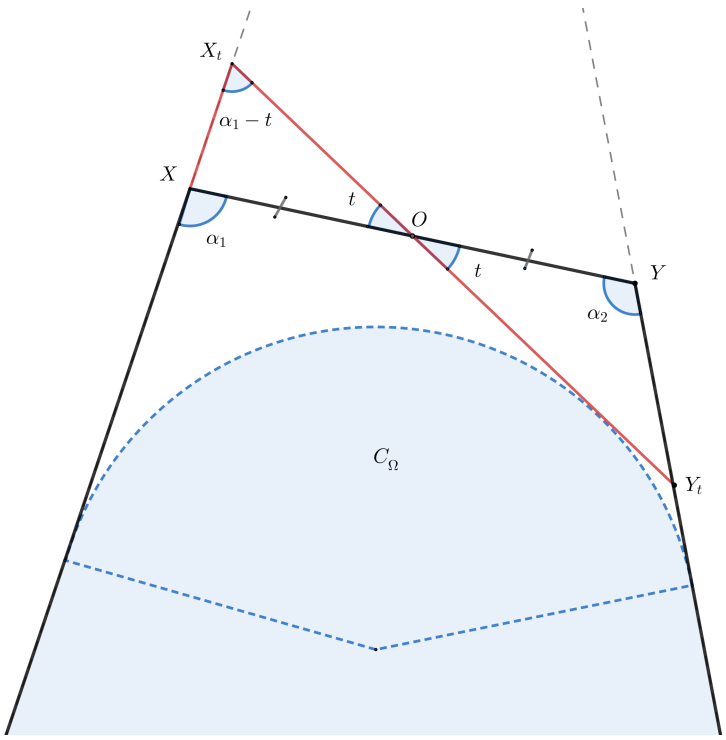

Figure 4: Rotation of the free side along its midpoint.

Without loss of generality, we assume that $\alpha_2 \geq \alpha_1$ and we take $t \in (0, \pi - \alpha_2)$. It is trivial that Ω and Ω_t have the same Cheeger constant, moreover if the side $[XY]$ is not touching ∂C_Ω then $\alpha_1 + \alpha_2 \geq \pi$ (see [26, Section 5]).

Let us now prove the inequalities $|\Omega_t| \leq |\Omega|$ and $P(\Omega_t) \geq P(\Omega)$. By using the sinus formula on the triangles OXX_t and OYY_t, we have

$$XX_t = a\frac{\sin t}{\sin(\alpha_1 - t)}, \qquad OX_t = a\frac{\sin \alpha_1}{\sin(\alpha_1 - t)}, \qquad YY_t = a\frac{\sin t}{\sin(\alpha_2 + t)} \qquad \text{and} \qquad OY_t = a\frac{\sin \alpha_2}{\sin(\alpha_2 + t)},$$

where $a := OX = XY/2$.

[4]We are thankful to Dorin Bucur for suggesting such deformations.

Moreover, if we denote by $\mathcal{S}_{OXX_t}$ and $\mathcal{S}_{OYY_t}$ the areas of the triangles OXX_t and OYY_t, we have

$$\begin{aligned}
|\Omega_t| - |\Omega| &= \mathcal{S}_{OXX_t} - \mathcal{S}_{OYY_t} \\
&= \frac{1}{2} OX \cdot OX_t \sin t - \frac{1}{2} OY \cdot OY_t \sin t \\
&= \frac{a^2}{2} \left(\frac{\sin \alpha_1}{\sin(\alpha_1 - t)} - \frac{\sin \alpha_2}{\sin(\alpha_2 + t)} \right) \sin t \\
&= \frac{a^2 \sin^2(t) \sin(\alpha_1 + \alpha_2)}{2 \sin(\alpha_1 - t) \sin(\alpha_2 + t)} \leq 0,
\end{aligned}$$

because $\alpha_1 + \alpha_2 \in [\pi, 2\pi]$, while $\alpha_1 - t$ and $\alpha_2 + t$ are in $(0, \pi]$.

For the perimeters, we have

$$\begin{aligned}
P(\Omega_t) - P(\Omega) &= XX_t + OX_t + OY_t - XY - YY_t \\
&= a \left(\frac{\sin t}{\sin(\alpha_1 - t)} + \frac{\sin \alpha_1}{\sin(\alpha_1 - t)} + \frac{\sin \alpha_2}{\sin(\alpha_2 + t)} - 2 - \frac{\sin t}{\sin(\alpha_2 + t)} \right) \\
&= a \left(\frac{\sin t + \sin \alpha_1}{\sin(\alpha_1 - t)} + \frac{\sin \alpha_2 - \sin t}{\sin(\alpha_2 + t)} - 2 \right) \\
&\geq a \left(\frac{\sin t + \sin \alpha_1}{\sin(\alpha_1 - t)} + \frac{\sin \alpha_1 - \sin t}{\sin(\alpha_1 + t)} - 2 \right) \\
&= a \left(\frac{2 \sin\left(\frac{\alpha_1 + t}{2}\right) \cos\left(\frac{\alpha_1 - t}{2}\right)}{2 \sin\left(\frac{\alpha_1 - t}{2}\right) \cos\left(\frac{\alpha_1 - t}{2}\right)} + \frac{2 \sin\left(\frac{\alpha_1 - t}{2}\right) \cos\left(\frac{\alpha_1 + t}{2}\right)}{2 \sin\left(\frac{\alpha_1 + t}{2}\right) \cos\left(\frac{\alpha_1 + t}{2}\right)} - 2 \right) \\
&= a \left(\sqrt{\frac{\sin\left(\frac{\alpha_1 + t}{2}\right)}{\sin\left(\frac{\alpha_1 - t}{2}\right)}} - \sqrt{\frac{\sin\left(\frac{\alpha_1 - t}{2}\right)}{\sin\left(\frac{\alpha_1 + t}{2}\right)}} \right)^2 \\
&\geq 0,
\end{aligned}$$

where the inequality in the middle is a consequence of the assumption $\alpha_1 \leq \alpha_2$ and the monotonicity of the function $g_t : x \longmapsto \frac{\sin x - \sin t}{\sin(x+t)}$ on $[\alpha_1, \alpha_2]$, where $t \in (0, \pi - \alpha_2)$. Indeed, we have for every $x \in [\alpha_1, \alpha_2]$

$$\begin{aligned}
g_t'(x) &= \frac{\cos x \sin(x + t) - (\sin x - \sin t) \cos(x + t)}{\sin^2(x + t)} \\
&= \frac{(\cos x \sin(x + t) - \sin x \cos(x + t)) + \sin t \cos(x + t)}{\sin^2(x + t)} \\
&= \frac{\sin t + \sin t \cos(x + t)}{\sin^2(x + t)} \\
&= \frac{\sin t \cdot (1 + \cos(x + t))}{\sin^2(x + t)} \\
&\geq 0.
\end{aligned}$$

Iterating, in a finite number of steps, we get a Cheeger-regular polygon $\tilde{\Omega}$ such that $|\Omega| \geq |\widetilde{\Omega}|$, $P(\Omega) \leq P(\widetilde{\Omega})$ and $h(\Omega) = h(\widetilde{\Omega})$.

□

In the following lemmas, we give some quantitative estimates for the perimeter, the Cheeger constant and the area via the Hausdorff distance and the radial functions (see Definition 13). These inequalities are used in the fourth step of Section 3.2.

Lemma 19. *If Ω_1 and Ω_2 are two planar convex sets, we have*

$$|P(\Omega_1) - P(\Omega_2)| \leq 2\pi d^H(\Omega_1, \Omega_2). \tag{15}$$

Proof. Let us respectively denote by h_{Ω_1} and h_{Ω_2} the support functions of Ω_1 and Ω_2, see Definition 13. We have

$$|P(\Omega_1) - P(\Omega_2)| = \left| \int_0^{2\pi} h_{\Omega_1} - \int_0^{2\pi} h_{\Omega_2} \right| \leq 2\pi \left\| h_{\Omega_1} - h_{\Omega_2} \right\|_\infty = 2\pi d^H(\Omega_1, \Omega_2),$$

where $\| \cdot \|_\infty$ stands for the infinity norm over $[0, 2\pi)$. □

Lemma 20. *Take Ω_1 and Ω_2 two planar domains starshaped with respect to the origin 0, whose radial functions are denoted by f_{Ω_1} and f_{Ω_2} and such that $f_{\Omega_1}, f_{\Omega_2} \geq r_0$, where $r_0 > 0$. We have*

1. $|h(\Omega_1) - h(\Omega_2)| \leq \frac{2}{r_0^2}\|f_{\Omega_1} - f_{\Omega_2}\|_\infty$,
2. $\big||\Omega_1| - |\Omega_2|\big| \leq 2\pi \max(\|f_{\Omega_1}\|_\infty, \|f_{\Omega_2}\|_\infty)\|f_{\Omega_1} - f_{\Omega_2}\|_\infty$,

where $\|\cdot\|_\infty$ stands for the infinity norm over $[0, 2\pi)$.

Proof. 1. The proof of this assertion is inspired from the proof of [15, Proposition 1].

Let us take $d := \|f_{\Omega_1} - f_{\Omega_2}\|_\infty$. We have for every $\theta \in [0, 2\pi)$

$$\left(1 + \frac{d}{r_0}\right) f_{\Omega_1}(\theta) = f_{\Omega_1}(\theta) + \frac{d}{r_0} f_{\Omega_1}(\theta) \geq f_{\Omega_1}(\theta) + d \geq f_{\Omega_1}(\theta) + f_{\Omega_2}(\theta) - f_{\Omega_1}(\theta) = f_{\Omega_2}(\theta).$$

Thus, $\Omega_2 \subset \left(1 + \frac{d}{r_0}\right)\Omega_1$, which implies the following

$$h(\Omega_1) \leq h\left(\frac{1}{1 + d/r_0}\Omega_2\right) = \left(1 + \frac{d}{r_0}\right) h(\Omega_2) \leq h(\Omega_2) + \frac{d}{r_0} h(B_{r_0}) = h(\Omega_2) + \frac{2d}{r_0^2},$$

where B_{r_0} is the disk of radius r_0. By similar arguments we obtain

$$h(\Omega_2) \leq h(\Omega_1) + \frac{2d}{r_0^2},$$

which proves the announced inequality.

2. We have

$$\begin{aligned}
\big||\Omega_1| - |\Omega_2|\big| &= \frac{1}{2}\left|\int_0^{2\pi} (f_{\Omega_1}^2(\theta) - f_{\Omega_2}^2(\theta))d\theta\right| \\
&\leq \frac{1}{2}\int_0^{2\pi} (|f_{\Omega_1}(\theta)| + |f_{\Omega_2}(\theta)|)|f_{\Omega_1}(\theta) - f_{\Omega_2}(\theta)|d\theta \\
&\leq 2\pi \max(\|f_{\Omega_1}\|_\infty, \|f_{\Omega_2}\|_\infty)\|f_{\Omega_1} - f_{\Omega_2}\|_\infty.
\end{aligned}$$

□

3 Proofs of the main results

3.1 Proof of the inequality (5)

The proof is done in four steps:

Step 1: Cheeger-regular polygons

Even-though the inequality was already known in this case, we briefly recall the proof for the sake of completeness. Since Ω is a Cheeger-regular polygon, by Theorem 11, we have an explicit formula of its Cheeger constant. We then use the inequality $T(\Omega) \leq \frac{P(\Omega)^2}{4|\Omega|}$ of Theorem 6 to conclude (see (8) for the definition of $T(\Omega)$). We write

$$h(\Omega) = \frac{P(\Omega) + \sqrt{P(\Omega)^2 - 4\big(T(\Omega) - \pi\big)|\Omega|}}{2|\Omega|} \geq \frac{P(\Omega) + \sqrt{P(\Omega)^2 - 4\left(\frac{P(\Omega)^2}{4|\Omega|} - \pi\right)|\Omega|}}{2|\Omega|} = \frac{P(\Omega) + \sqrt{4\pi|\Omega|}}{2|\Omega|}.$$

Step 2: General polygons

By Lemma 18, there exists $\widetilde{\Omega}$ a Cheeger-regular polygon such that $|\Omega| \geq |\widetilde{\Omega}|$, $P(\Omega) \leq P\big(\widetilde{\Omega}\big)$ and $h(\Omega) = h\big(\widetilde{\Omega}\big)$. Then, we get

$$h(\Omega) = h\big(\widetilde{\Omega}\big) \geq \frac{P\left(\widetilde{\Omega}\right) + \sqrt{4\pi\left|\widetilde{\Omega}\right|}}{2\left|\widetilde{\Omega}\right|} = \frac{P\big(\widetilde{\Omega}\big)}{2\left|\widetilde{\Omega}\right|} + \frac{\pi}{\sqrt{\left|\widetilde{\Omega}\right|}} \geq \frac{P(\Omega)}{2|\Omega|} + \frac{\pi}{\sqrt{|\Omega|}} = \frac{P(\Omega) + \sqrt{4\pi|\Omega|}}{2|\Omega|}.$$

Step 3: General convex sets

By the density of the polygons in $\mathcal{K}^2$ and the continuity of the area, the perimeter and the Cheeger constant with respect to the Hausdorff distance, we show that the inequality (5) holds for general convex sets. We refer to [32, Proposition 3.1] for the continuity of the Cheeger constant with respect to the Hausdorff distance in the class of convex sets.

Step 4: Equality for sets that are homothetical to their form bodies

If Ω is homothetical to its form body (which is the case for circumscribed polygons), we have by using [36, Equality (7.168)] and the equality $\frac{1}{2}r(\Omega)P(\Omega) = |\Omega|$ (see for example [2])

$$\forall t \in [0, r(\Omega)], \quad |\Omega_{-t}| = \left(1 - \frac{t}{r(\Omega)}\right)^2 |\Omega| = |\Omega| - P(\Omega)t + \frac{P(\Omega)^2}{4|\Omega|}t^2.$$

The equation $|\Omega_{-t}| = \pi t^2$ admits two different solutions $\frac{2|\Omega|}{P(\Omega)-\sqrt{4\pi|\Omega|}}$ and $\frac{2|\Omega|}{P(\Omega)+\sqrt{4\pi|\Omega|}}$. Thus, by Theorem 10 we have

$$h(\Omega) \in \left\{ \frac{P(\Omega) - \sqrt{4\pi|\Omega|}}{2|\Omega|}, \frac{P(\Omega) + \sqrt{4\pi|\Omega|}}{2|\Omega|} \right\}.$$

At last, since $h(\Omega) \geq \frac{P(\Omega)+\sqrt{4\pi|\Omega|}}{2|\Omega|} > \frac{P(\Omega)-\sqrt{4\pi|\Omega|}}{2|\Omega|}$ (by inequality (5)), we deduce the equality

$$h(\Omega) = \frac{P(\Omega) + \sqrt{4\pi|\Omega|}}{2|\Omega|}. \tag{16}$$

3.2 Proof of the second assertion of Theorem 2 (convex sets)

The inequalities (3) and (5) (stated in the introduction) imply that

$$\mathcal{D}_{\mathcal{K}^2} \subset \left\{ (x, y) \ \mid \ x \geq x_0 \ \text{ and } \ \frac{1}{2}x + \sqrt{\pi} \leq y \leq x \right\}.$$

It remains to prove the opposite inclusion. The proof follows the following steps:

1. We provide a continuous family $(S_p)_{p \geq P(B)}$ of convex bodies which fill the upper boundary of the diagram.
2. We provide a continuous family $(L_p)_{p \geq P(B)}$ of convex bodies which fill the lower boundary of the diagram.
3. We use the latter domains to construct (via Minkowski sums) a family of continuous paths $(\Gamma_p)_{p \geq P(B)}$ which relate the upper domains to the lower ones. By continuously increasing the perimeter, we show that we are able to cover all the area between the upper and lower boundaries of the diagram $\mathcal{D}_{\mathcal{K}^2}$ (see Definition 3 for the notion of upper and lower boundaries of the diagram $\mathcal{D}_{\mathcal{K}^2}$).

Step 1: The upper boundary of the diagram $\mathcal{D}_{\mathcal{K}^2}$:

The upper boundary of $\mathcal{D}_{\mathcal{K}^2}$ (see Definition 3) is filled by domains that are Cheeger of themselves, which means that $C_\Omega = \Omega$. It is shown in [26, Theorem 2] that the stadiums (i.e., the convex hull of two identical disks) are Cheeger of themselves. We then use these sets to fill the upper boundary $\{(x, x) \mid x \geq P(B)\}$.

Let us consider the family of stadiums $(Q_t)_{t \geq 0}$ given by the convex hulls of the balls of unit radius centered in $O(0, 0)$ and $O_t(0, t)$ rescaled so as $|Q_t| = 1$. The function $t \in [0, +\infty) \longmapsto P(Q_t) = \frac{2(\pi+t)}{\sqrt{\pi+2t}}$ is continuous and strictly increasing to infinity. Thus, we have by the Intermediate Value Theorem

$$\big\{\big(P(Q_t), h(Q_t)\big) \mid t \geq 0\big\} = \big\{\big(P(Q_t), P(Q_t)\big) \mid t \geq 0\big\} = \{(x, x) \mid x \geq P(B)\}.$$

Step 2: The lower boundary of the diagram $\mathcal{D}_{\mathcal{K}^2}$:

Since the equality (16) holds for sets that are homothetical to their form bodies, we use such domains to fill the lower boundary. Let us consider the family $(C_d)_{d \geq 2}$ of the so-called symmetrical cup-bodies, which are given by the convex hulls of the unit ball (centered in $O(0, 0)$) and the points of coordinates $(-d/2, 0)$ and $(d/2, 0)$ rescaled so as $|C_d| = 1$. By using formulas (7) and (8) of [23], we have for every $d \geq 2$

$$P(C_d) = 2\sqrt{\sqrt{d^2 - 4} + 2\arcsin\left(\frac{2}{d}\right)}.$$

The function $d \in [2,+\infty) \longmapsto P(C_d) = 2\sqrt{\sqrt{d^2-4} + 2\arcsin\left(\frac{2}{d}\right)}$ is continuous and strictly increasing to infinity. Thus, we have by the Intermediate Value Theorem

$$\{\big(P(C_d), h(C_d)\big) \mid d \geq 2\} = \{\big(P(C_d), P(C_d)/2 + \sqrt{\pi}\big) \mid d \geq 2\} = \{(x, x/2 + \sqrt{\pi}) \mid x \geq P(B)\}.$$

Step 3: Continuous paths:

Since the functions $t \in [0,+\infty) \longmapsto P(Q_t) = \frac{2(\pi+t)}{\sqrt{\pi+2t}}$ and $d \in [2,+\infty) \longmapsto P(C_d) = 2\sqrt{\sqrt{d^2-4} + 2\arcsin\frac{2}{d}}$ are continuous and strictly increasing, we have

$$\forall p \geq P(B), \exists!(t_p, d_p) \in [0,+\infty) \times [2,+\infty), \quad P(Q_{t_p}) = P(C_{d_p}) = p.$$

From now on we take $S_p := Q_{t_p}$ and $L_p := C_{d_p}$.

For every $p \geq P(B)$, we introduce the closed and continuous path $\Gamma_p : [0,3) \longrightarrow \mathbb{R}^2$, defined as follows:

$$t \quad \longmapsto \quad \begin{cases} \big(P(K_p^t), h(K_p^t)\big), & \text{if } t \in [0,1], \\ \big((t-1)P(B) + (2-t)p, (t-1)P(B) + (2-t)p\big), & \text{if } t \in (1,2], \\ \big((3-t)P(B) + (t-2)p,\ (3-t)P(B) + (t-2)(p/2 + \sqrt{\pi})\big)\big), & \text{if } t \in (2,3), \end{cases}$$

with

$$K_p^t := \frac{tS_p \oplus (1-t)L_p}{\sqrt{|tS_p \oplus (1-t)L_p|}} \in \mathcal{K}^2,$$

where $tS_p \oplus (1-t)L_p$ is the Minkowski sum of the sets tS_p and $(1-t)L_p$ (see Definition 8).

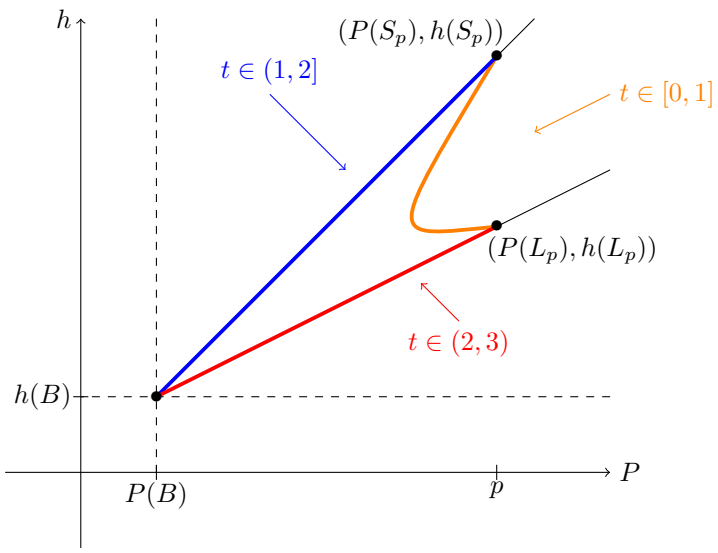

Figure 5: The continuous and closed path Γ_p

For every $t \in [0,1]$, the set K_p^t is convex with unit area. Moreover, by the continuity of the perimeter, the area and the Cheeger constant with respect to the Hausdorff distance, we have that the set $\{(P(K_p^t), h(K_p^t)) \mid t \in [0,1]\}$ is a continuous curve in $\mathbb{R}^2$. Thus, we conclude that the path Γ_p is a closed and continuous curve in $\mathbb{R}^2$.

Since the diameters of L_p and S_p are colinear, we can use the following result of **Step 3** of the proof of [21, Theorem 3.14]:

$$\forall t \in [0,1], \qquad \frac{p}{2} \leq P(K_p^t). \tag{17}$$

Step 4: Stability of the paths:

Now, let us prove a continuity result on the paths $\big(\Gamma_p\big)_{p \geq P(B)}$. We take $p_0 \geq P(B)$ and $\varepsilon > 0$, and show that

$$\exists\, \alpha_\varepsilon > 0, \forall p \in (p_0 - \alpha_\varepsilon, p_0 + \alpha_\varepsilon) \cap [P(B), +\infty), \qquad \sup_{t \in [0,3]} \| \Gamma_p(t) - \Gamma_{p_0}(t) \| \leq \varepsilon. \tag{18}$$

Let $p \in [P(B), p_0+1]$, with straightforward computations, we have that for every $t \in [1,3)$,

$$\|\Gamma_p(t) - \Gamma_{p_0}(t)\| \leq 2|p-p_0| \underset{p\to p_0}{\longrightarrow} 0.$$

The remaining case ($t \in [0,1]$) requires more computations. For every $t \in [0,1]$, we have

$$\|\Gamma_p(t) - \Gamma_{p_0}(t)\| \leq |P(K_p^t) - P(K_{p_0}^t)| + |h(K_p^t) - h(K_{p_0}^t)| \leq \underbrace{\left(2\pi + \frac{(p_0+1)^6}{2}\right)}_{C_{p_0}>0} d^H(K_p^t, K_{p_0}^t).$$

Indeed, we used:

- Lemma 19 for the term with the perimeters

$$|P(K_p^t) - P(K_{p_0}^t)| \leq 2\pi d^H(K_p^t, K_{p_0}^t),$$

- and the first assertion of Lemma 20 for the term with the Cheeger constants, with the sets K_p^t and $K_{p_0}^t$ that we assume to contain the origin 0 and whose radial functions (see Definition 13) are denoted by $f_{p,t}, f_{p_0,t}$.

$$\begin{aligned}
|h(K_p^t) - h(K_{p_0}^t)| &\leq \frac{2}{\min\left(r(K_p^t), r(K_{p_0}^t)\right)^2} \cdot \|f_{p,t} - f_{p_0,t}\|_\infty \quad \text{(by Lemma 20)} \\
&\leq \frac{2}{\min\left(r(K_p^t), r(K_{p_0}^t)\right)^2} \cdot \frac{\|f_{p,t}\|_\infty \|f_{p_0,t}\|_\infty}{\min\left(r(K_p^t), r(K_{p_0}^t)\right)^2} \cdot d^H(K_p^t, K_{p_0}^t) \quad \text{(by [6, Proposition 2])} \\
&\leq \frac{(p_0+1)^6}{2} d^H(K_p^t, K_{p_0}^t) \quad \text{(we used } \|f_\Omega\|_\infty \leq d(\Omega) \leq \frac{P(\Omega)}{2} \text{ and } r(\Omega) > \frac{|\Omega|}{P(\Omega)}\text{, see [8, Lemma B.1])}.
\end{aligned}$$

It remains to prove that $d^H(K_p^t, K_{p_0}^t)$ converges (uniformly in t) to 0 when p goes to p_0. Before detailing the computations, let us recall that if Ω is a convex body, we denote by h_Ω its support function defined in Definition 13 (we refer the reader to Remark 14 for some interesting properties of support functions). We also note that if $\Omega_1, \Omega_2 \in \mathcal{K}^2$ such that $|\Omega_1| = |\Omega_2| = 1$, one has

$$\forall t \in [0,1], \quad |(1-t)\Omega_1 \oplus t\Omega_2| \geq ((1-t)|\Omega_1|^{1/2} + t|\Omega_2|^{1/2})^2 = 1,$$

where we used the classical Brunn–Minkowski inequality (see [36, Theorem 7.1.1] for example). We are now in position to conclude.

$$\begin{aligned}
d^H(K_p^t, K_{p_0}^t) &= \left\| h_{K_p^t} - h_{K_{p_0}^t} \right\|_\infty \quad \text{(by [36, Lemma 1.8.14])} \\
&= \left\| \frac{(1-t)h_{L_{p_0}} + th_{S_{p_0}}}{\sqrt{|(1-t)L_{p_0} \oplus tS_{p_0}|}} - \frac{(1-t)h_{L_p} + th_{S_p}}{\sqrt{|(1-t)L_p \oplus tS_p|}} \right\|_\infty \\
&\leq (1-t) \left\| \frac{h_{L_{p_0}}}{\sqrt{|(1-t)L_{p_0} \oplus tS_{p_0}|}} - \frac{h_{L_p}}{\sqrt{|(1-t)L_p \oplus tS_p|}} \right\|_\infty \\
&\quad + t \left\| \frac{h_{S_{p_0}}}{\sqrt{|(1-t)L_{p_0} \oplus tS_{p_0}|}} - \frac{h_{S_p}}{\sqrt{|(1-t)L_p \oplus tS_p|}} \right\|_\infty \\
&\leq \frac{1}{\sqrt{|(1-t)L_p \oplus tS_p|}} \left(\left\| h_{S_{p_0}} - h_{S_p} \right\|_\infty + \left\| h_{L_{p_0}} - h_{L_p} \right\|_\infty \right) \\
&\quad + \left(\left\| h_{S_{p_0}} \right\|_\infty + \left\| h_{L_{p_0}} \right\|_\infty \right) \left| \frac{1}{\sqrt{|(1-t)L_p \oplus tS_p|}} - \frac{1}{\sqrt{|(1-t)L_{p_0} \oplus tS_{p_0}|}} \right| \\
&\leq d^H(S_{p_0}, S_p) + d^H(L_{p_0}, L_p) + \left(\left\| h_{S_{p_0}} \right\|_\infty + \left\| h_{L_{p_0}} \right\|_\infty \right) \Big| \, |(1-t)L_p \oplus tS_p| - |(1-t)L_{p_0} \oplus tS_{p_0}| \, \Big| \\
&\leq d^H(S_{p_0}, S_p) + d^H(L_{p_0}, L_p) + \left(\left\| h_{S_{p_0}} \right\|_\infty + \left\| h_{L_{p_0}} \right\|_\infty \right) \sum_{k=0}^{2} |W_k(L_p, S_p) - W_k(L_{p_0}, S_{p_0})| \underset{p\to p_0}{\longrightarrow} 0,
\end{aligned}$$

where W_0, W_1 and W_2 stand for the Minkowski mixed volumes introduced in Theorem 15.

Finally, we deduce that $\lim_{p\to p_0} \sup_{t\in[0,3]} \| \Gamma_p(t) - \Gamma_{p_0}(t)\| = 0$, which proves (18).

Step 5: Conclusion:

Now that we proved that the boundaries $\{(x,x) \mid x \geq P(B)\}$ and $\{(x, x/2+\sqrt{\pi}) \mid x \geq P(B)\}$ are included in the diagram $\mathcal{D}_{\mathcal{K}^2}$, it remains to show that it is also the case for the set of points contained between them. Let $A(x_A, y_A) \in \{(x,y) \mid x > x_0 \text{ and } x/2+\sqrt{\pi} < y < x\}$. Step 4 shows that for any choice of p_0 and p_1 in $[P(B), +\infty)$, the curves Γ_{p_0} and Γ_{p_1} are homotopic, and the homotopy is $H : (\sigma, t) \in [0,1] \times [0,3) \longmapsto \Gamma_{(1-\sigma)p_0+\sigma p_1}$. In particular, let us chose $p_0 = P(B)$ and $p_1 = 4x_A$. The index of A with respect to $\Gamma_{P(B)} = \{(P(B), P(B))\}$ is equal to 0. Meanwhile, by the inequality (17) of Step 3, we deduce that A is in the interior of the curve Γ_{4x_A}, which means that its index with respect to Γ_{4x_A} is non-zero. Thus, it must follow that there exists $(\bar{\sigma}, \bar{t}) \in [0,1] \times [0,3)$ such that $A = H(\bar{\sigma}, \bar{t}) \in \mathcal{D}_{\mathcal{K}^2}$.

Finally, we get the equality

$$\mathcal{D}_{\mathcal{K}^2} = \left\{(x,y) \mid x \geq x_0 \text{ and } \frac{1}{2}x + \sqrt{\pi} \leq y \leq x\right\}.$$

3.3 Proof of the first assertion of Theorem 2 (simply connected sets)

By the inequalities (3) and (4) where the latter one is an equality if and only if Ω is a ball, we have

$$\mathcal{D}_{\mathcal{S}^2} \subset \{(x_0, x_0)\} \cup \{(x,y) \mid x > x_0 \text{ and } x_0 < y \leq x\}.$$

We have $(x_0, x_0) = \big(P(B), h(B)\big) \in \mathcal{D}_{\mathcal{S}^2}$. Take $(p, \ell) \in \{(x,y) \mid x > x_0 \text{ and } x_0 < y \leq x\}$, let us prove that there exists a simply connected domain $\Omega \subset \mathbb{R}^2$ of unit area such that $P(\Omega) = p$ and $h(\Omega) = \ell$.

If $\ell \geq p/2 + \sqrt{\pi}$, then by the second assertion of Theorem 2 there exists a convex (thus simply connected) domain satisfying the latter properties. Now, let us assume that $\ell < p/2 + \sqrt{\pi}$. We take $L_{2(\ell-\sqrt{\pi})}$ as in the proof of the second assertion of Theorem 2 (see Step 3 of Section 3.2) to be a symmetrical 2-cup body (which is the convex hull of a disk and two points outside it that are symmetric with respect to its center) such that $P(L_{2(\ell-\sqrt{\pi})}) = 2(\ell - \sqrt{\pi}) < p$, $|L_{2(\ell-\sqrt{\pi})}| = 1$ and $h(L_{2(\ell-\sqrt{\pi})}) = \ell$ (where we used the equality (16) since $L_{2(\ell-\sqrt{\pi})}$ is homothetical to its form body). Since, the involved functionals are invariant with respect to translations and rotations, we may assume without loss of generality that $L_{2(\ell-\sqrt{\pi})}$ is symmetric with respect to the x-axis, included $\{x \leq 0\}$ and its boundary touches the y-axis in the origin 0 which is assumed to be a singular point, see Figure 6. Let $\varepsilon > 0$ sufficiently small such that the set C_ℓ (the Cheeger set of $L_{2(\ell-\sqrt{\pi})}$) is included in the half-plane $\{x < -\varepsilon\}$. We denote by $A(-\varepsilon, c_\varepsilon)$ and $B(-\varepsilon, -c_\varepsilon)$, where $c_\varepsilon > 0$, the points of the intersection between the line $\{x = -\varepsilon\}$ and the boundary of $L_{2(\ell-\sqrt{\pi})}$ (see Figure 6). For $t \geq 0$, we introduce the points $A_t\left(-\varepsilon, \frac{\varepsilon c_\varepsilon}{\varepsilon+t}\right)$, $B_t\left(-\varepsilon, -\frac{\varepsilon c_\varepsilon}{\varepsilon+t}\right)$ and $O_t\,(t, 0)$. We then define for every $t \geq 0$,

$$L^t := (L_{2(\ell-\sqrt{\pi})} \cap \{x \leq -\varepsilon\}) \cup \mathcal{T}_t,$$

where $\mathcal{T}_t$ is the (closed) triangle of vertices O_t, A_t and B_t. The function $t \geq 0 \longmapsto P(L^t)$ continuously varies from $2(\ell - \sqrt{\pi})$ to $+\infty$. Thus, by the Intermediate Value Theorem, there exists t_p such that $P(L^{t_p}) = p$. Moreover, the set L^{t_p} is simply connected with unit area and has the same Cheeger set as $L_{2(\ell-\sqrt{\pi})}$, which yields that $h(L^{t_p}) = h(L_{2(\ell-\sqrt{\pi})}) = \ell$. This shows that $(p, \ell) \in \mathcal{D}_{\mathcal{S}^2}$.

Finally, we obtain the equality

$$\mathcal{D}_{\mathcal{S}^2} = \{(x_0, x_0)\} \cup \{(x,y) \mid x > x_0 \text{ and } x_0 < y \leq x\}.$$

3.4 Proof of the inequality (7)

This is a direct application of Lemma 16 and the inequality $T(\Omega) \geq N \tan \frac{\pi}{N}$ (see Theorem 6 and (8) for the definition of $T(\Omega)$). Indeed, for any $\Omega \in \mathcal{P}_N$, one has

$$h(\Omega) \leq \frac{P(\Omega) + \sqrt{P(\Omega)^2 - 4\big(T(\Omega) - \pi\big)|\Omega|}}{2|\Omega|} \leq \frac{P(\Omega) + \sqrt{P(\Omega)^2 + 4\big(\pi - N\tan\frac{\pi}{N}\big)|\Omega|}}{2|\Omega|}.$$

The first inequality is an equality if and only if Ω is Cheeger-regular and the second one is an equality if and only if $T(\Omega) = N \tan \frac{\pi}{N}$, which is equivalent to $\alpha_1 = \cdots = \alpha_N = \frac{N-2}{N}\pi$.

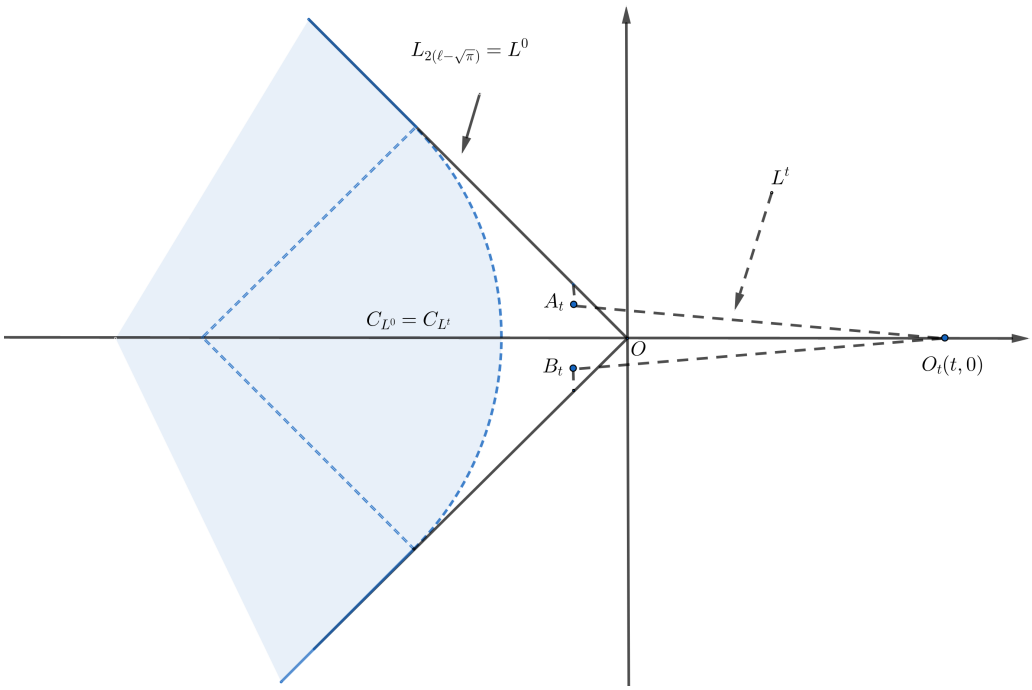

Figure 6: Tailed domain L^t with the same area, the same Cheeger set and higher perimeter.

3.5 Proof of Theorem 5

3.5.1 If $N = 3$

We have by (6),

$$\forall \Omega \in \mathcal{P}_3, \qquad \sqrt{|\Omega|}h(\Omega) = \frac{P(\Omega)}{2\sqrt{|\Omega|}} + \sqrt{\pi}.$$

Thus, we have the inclusion

$$\mathcal{D}_3 \subset \left\{ \left(x, \frac{x}{2} + \sqrt{\pi}\right) \,\middle|\, x \geq P(R_3) \right\}.$$

The opposite inclusion is proved by considering for example the family $(T_d)_{d\geq 1}$ of isosceles triangles of vertices $X_d\left(0, \frac{\sqrt{3}}{2}\right)$, $Y_d\left(\frac{d}{2}, 0\right)$ and $Z_d\left(-\frac{d}{2}, 0\right)$. We have for every $d \geq 1$,

$$\begin{cases} P(R_3) = x_1 \leq x_d := \frac{P(T_d)}{\sqrt{|T_d|}} = \frac{d+\sqrt{d^2+3}}{\frac{3^{1/4}}{2}\sqrt{d}} \underset{d\to+\infty}{\longrightarrow} +\infty \\ h(R_3) = y_1 \leq y_d := \frac{P(T_d)}{2\sqrt{|T_d|}} + \sqrt{\pi} = \frac{d+\sqrt{d^2+3}}{3^{1/4}\sqrt{d}} + \sqrt{\pi} \underset{d\to+\infty}{\longrightarrow} +\infty, \end{cases}$$

where the inequalities $x_1 \leq x_d$ and $y_1 \leq y_d$ are consequences of the isoperimetric inequality for triangles.

3.5.2 If N is even

We have by the inequalities (5) and (7)

$$\mathcal{D}_N \subset \left\{ (x,y) \mid x \geq P(R_N) \text{ and } \frac{x}{2} + \sqrt{\pi} \leq y \leq f_N(x) \right\},$$

where $f_N : x \in [P(R_N), +\infty) \longmapsto \frac{x+\sqrt{x^2+4(\pi - N\tan\frac{\pi}{N})}}{2}$.

It remains to prove the opposite inclusion. We provide explicit families of elements of $\mathcal{P}_N$ that respectively fill the upper and lower boundaries of $\mathcal{D}_N$ (see Definition 4) and then use those domains to construct continuous paths that fill the diagram.

Step 1: The upper boundary of $\mathcal{D}_N$:

We recall that the inequality (7) is an equality if and only if Ω is Cheeger-regular and all its angles are equal to $(N-2)\pi/N$. We assume without loss of generality that two parallel sides of the regular N-gon R_N are colinear to

the x-axis (note that this is possible because the number of sides N is even). We then consider the family of N-gons $(\widetilde{U}_t)_{t\geq 1}$ such that for every $t \geq 1$,

$$\widetilde{U}_t := \{(tx, y) \mid (x, y) \in R_N\}.$$

Since the map $t \geq 1 \longmapsto d(\widetilde{U}_t) \geq d(R_N)$ is continuous and strictly increasing, it is a bijection. Thus, for every $\delta \geq d(R_N)$, there exists a unique $t_\delta \geq 1$ such that $d(\widetilde{U}_{t_\delta}) = \delta$. From now on we denote $U_\delta := \widetilde{U}_{t_\delta}$ for every $\delta \geq d(R_N)$.

Since

- $(U_\delta)_\delta$ is a family of N-gons that vary continuously with respect to the Hausdorff distance,
- the perimeter and the area are continuous with respect to the Hausdorff distance,
- $P(U_{d(R_N)}) = P(R_N)$ and

$$\frac{P(U_\delta)}{|U_\delta|^{1/2}} \geq \frac{P(U_\delta)}{\delta^{1/2} d(R_N)^{1/2}} \geq \frac{2\delta}{\delta^{1/2} d(R_N)^{1/2}} = \frac{2}{d(R_N)^{1/2}} \delta^{1/2} \underset{\delta \to +\infty}{\longrightarrow} +\infty, \tag{19}$$

we have by the Intermediate Value Theorem:

$$\forall\, p \geq P(R_N), \exists\, \delta_p \geq d(R_N), \qquad \frac{P(U_{\delta_p})}{|U_{\delta_p}|^{1/2}} = p.$$

Moreover, the sets (U_δ) are Cheeger-regular and all their interior angles are equal to $(N-2)\pi/N$. Thus, they all realize the equality

$$|U_\delta|^{1/2} h(U_\delta) = \frac{P(U_\delta) + \sqrt{P(U_\delta)^2 + 4\big(\pi - N \tan \frac{\pi}{N}\big)|U_\delta|}}{2|U_\delta|^{1/2}} = f_N\left(\frac{P(U_\delta)}{\sqrt{|U_\delta|}}\right).$$

We then deduce that the upper boundary of $\mathcal{D}_N$ is given by the set of points $\big\{\big(x, f_N(x)\big) \mid x \geq P(R_N)\big\}$.

Step 2: The lower boundary of $\mathcal{D}_N$:

As for the upper boundary's case, we construct a continuous family of N-gons $(V_\delta)_{\delta \geq d(R_N)}$, such that $V_{d(R_N)} = R_N$ and $d(V_\delta) = \delta$ for every $\delta \geq d(R_N)$. We assume that a diameter of R_N is given by $[OA]$, where $O = (0,0)$ and $A = (d(R_N), 0)$ and denote by B_N its incircle (see Figure 7) and $M_1, \ldots, M_N$ its vertices.

Take $\delta \geq d(R_N)$, we denote by $A_\delta = (\delta, 0)$ and $(\Delta_\delta), (\Delta'_\delta)$ the lines passing through A_δ which are tangent to B_N. The line (Δ_δ) (resp. (Δ'_δ)) cuts the boundary of R_N in at least two points: we denote by $M^\delta_{k_\delta}$ (resp. $M^\delta_{N-k_\delta+1}$) the farthest one from A_δ (see Figure 7), where $k_\delta \in [\![1, N/2]\!]$ such that $2k_\delta$ is the number of vertices of R_N that are in the region given by the convex cone delimited by (Δ_δ) and (Δ'_δ). We then define V_δ as the (convex) polygon whose vertices are given by

$$\begin{cases} M^\delta_1 = M_1 = O, \\ M^\delta_i = M_i, \quad \text{for all } k \in [\![2, k_\delta - 1]\!] \\ M^\delta_{k_\delta} = \cdots = M^\delta_{\frac{N}{2}} \\ M^\delta_{\frac{N}{2}+1} = A_\delta \\ M^\delta_{\frac{N}{2}+2} = \cdots = M^\delta_{N+2-k_\delta} \\ M^\delta_i = M_i \quad \text{for all } k \in [\![N+2-k_\delta, N-1]\!] \end{cases}$$

Note that V_δ has at most N sides and that it is a circumscribed polygon. This yields that the couple $(\frac{P(V_\delta)}{|V_\delta|^{1/2}}, |V_\delta|^{1/2} h(V_\delta))$ lies on the lower boundary of the diagram $\mathcal{D}_N$. We also, note that the applications $\delta \in [d(R_N), +\infty) \longmapsto M^\delta_k \in \mathbb{R}^2$ are continuous and thus the family of polygons $(V_\delta)_\delta$ is continuous with respect to the Hausdorff distance. Then, by estimates similar to (19), we get that $\lim\limits_{\delta \to +\infty} \frac{P(V_\delta)}{|V_\delta|^{1/2}} = +\infty$. Thus, the lower boundary of $\mathcal{D}_N$ is given by the set of points $\big\{\big(x, x/2 + \sqrt{\pi}\big) \mid x \geq P(R_N)\big\}$.

Step 3: Continuous paths:

Now that we have two families (U_δ) and (V_δ) of extremal shapes, it remains to define continuous paths that connect the upper domains to the lower ones and fill the whole diagram. Unfortunately, unlike for the case of the class $\mathcal{K}^2$,

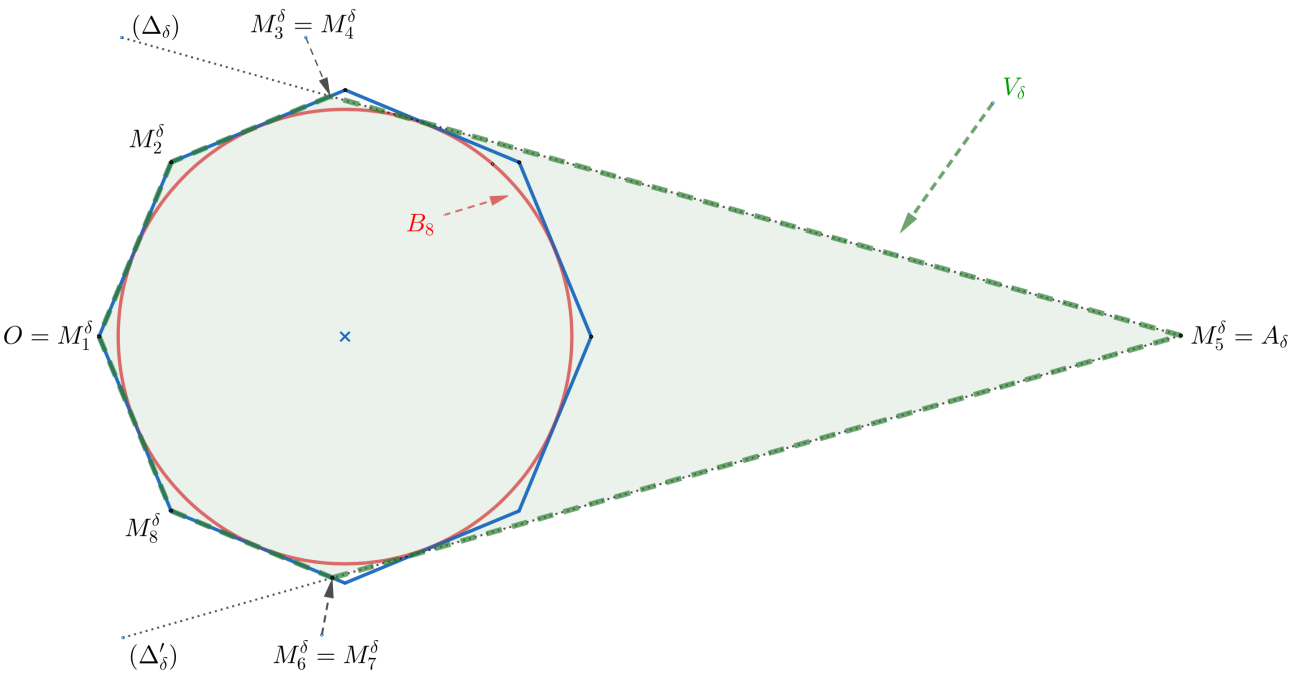

Figure 7: Construction of the circumscribed polygons V_δ for $N = 8$.

one cannot use Minkowski sums as they increase the number of sides and thus could give polygons that are not in the class $\mathcal{P}_N$, we will then construct the paths by continuously mapping the lower and upper polygons vertices.

We assume without loss of generality that as for V_δ the diameter of U_δ is given by OA_δ. We denote by $O = L_1^\delta, L_2^\delta, \dots, L_{N/2-1}^\delta = A_\delta, L_{N/2}^\delta, \dots, L_N^\delta$ the vertices of U_δ. For $t \in [0,1]$, we define Ω_t^δ as the polygon of vertices $((1-t)M_k^\delta + tL_k^\delta)_{k\in[\![1,N]\!]}$. The polygon Ω_t^δ is convex and included in the rectangle $(0,\delta) \times \left(-\frac{d(R_N)}{2}, \frac{d(R_N)}{2}\right)$. Thus, we have the following inequality :

$$\forall t \in [0,1], \qquad \frac{P(\Omega_t^\delta)}{|\Omega_t^\delta|^{1/2}} \geq \frac{2\delta}{\delta^{1/2} d(R_N)^{1/2}} = \frac{2}{d(R_N)^{1/2}} \delta^{1/2}. \tag{20}$$

For every $\delta \geq d(R_N)$, we introduce the closed and continuous path $\gamma_\delta : [0,3) \longrightarrow \mathbb{R}^2$, defined as follows:

$$t \quad \longmapsto \quad \begin{cases} \left(\frac{P(\Omega_t^\delta)}{|\Omega_t^\delta|^{1/2}}, |\Omega_t^\delta|^{1/2} h(\Omega_t^\delta)\right), & \text{if } t \in [0,1], \\ \left((t-1)P(R_N) + (2-t)\frac{P(U_\delta)}{|U_\delta|^{1/2}}\ ,\ f_N\left((t-1)P(R_N) + (2-t)\frac{P(U_\delta)}{|U_\delta|^{1/2}}\right)\right), & \text{if } t \in (1,2], \\ \left((3-t)P(R_N) + (t-2)\frac{P(V_\delta)}{|V_\delta|^{1/2}}\ ,\ (3-t)(\frac{P(R_N)}{2} + \sqrt{\pi}) + (t-2)(\frac{P(V_\delta)}{2|V_\delta|^{1/2}} + \sqrt{\pi})\right), & \text{if } t \in (2,3). \end{cases}$$

Step 4: Stability of the paths:

Take $\delta_0 \geq d(R_N)$ and $\varepsilon > 0$, let us show that

$$\exists\, \alpha_\varepsilon > 0, \forall \delta \in (\delta_0 - \alpha_\varepsilon, \delta_0 + \alpha_\varepsilon) \cap [P(R_N), +\infty), \qquad \sup_{t\in[0,3]} \| \gamma_\delta(t) - \gamma_{\delta_0}(t) \| \leq \varepsilon. \tag{21}$$

Let us take $\delta \in [d(R_N), \delta_0 + 1]$, with straightforward computations, there exists a constant $C(\delta_0) > 0$ depending only on δ_0 such that for every $t \in [1,3]$,

$$\|\gamma_\delta(t) - \gamma_{\delta_0}(t)\| \leq C(\delta_0) \min\left(\left|\frac{P(U_\delta)}{|U_\delta|^{1/2}} - \frac{P(U_{\delta_0})}{|U_{\delta_0}|^{1/2}}\right|, \left|\frac{P(V_\delta)}{|V_\delta|^{1/2}} - \frac{P(V_{\delta_0})}{|V_{\delta_0}|^{1/2}}\right|\right) \underset{\delta\to\delta_0}{\longrightarrow} 0.$$

Moreover, by the quantitative estimates given in Lemma 20, there exist constants $C'(\delta_0), C''(\delta_0) > 0$, depending

only on δ_0, such that for all $\delta \in [d(R_N), \delta_0 + 1]$ and all $t \in [0,1]$

$$\begin{aligned}
\|\gamma_\delta(t) - \gamma_{\delta_0}(t)\| &\leq \left| \frac{P(\Omega_t^\delta)}{|\Omega_t^\delta|^{1/2}} - \frac{P(\Omega_t^{\delta_0})}{|\Omega_t^{\delta_0}|^{1/2}} \right| + \left| |\Omega_t^\delta|^{1/2} h(\Omega_t^\delta) - |\Omega_t^{\delta_0}|^{1/2} h(\Omega_t^{\delta_0}) \right| \\
&\leq C'(\delta_0) \left(|P(\Omega_t^\delta) - P(\Omega_t^{\delta_0})| + \left| |\Omega_t^\delta| - |\Omega_t^{\delta_0}| \right| + |h(\Omega_t^\delta) - h(\Omega_t^{\delta_0})| \right) \\
&\leq C''(\delta_0) \max_{i \in [\![1,N]\!]} \|(1-t)M_i^\delta + tL_i^\delta - (1-t)M_i^{\delta_0} - tL_i^{\delta_0}\| \\
&\leq C''(\delta_0) \max_{i \in [\![1,N]\!]} (\|M_i^\delta - M_i^{\delta_0}\| + \|L_i^\delta - L_i^{\delta_0}\|) \underset{\delta \to \delta_0}{\longrightarrow} 0.
\end{aligned}$$

Finally, we deduce that $\lim_{\delta \to \delta_0} \sup_{t \in [0,3]} \| \gamma_\delta(t) - \gamma_{\delta_0}(t)\| = 0$, which proves (21).

Step 5: Conclusion:

As for the case of convex sets (see Section 3.2), now that we proved that the boundaries $\{\big(x, f_N(x)\big) \mid x \geq P(R_N)\}$ and $\{(x, x/2+\sqrt{\pi}) \mid x \geq P(R_N)\}$ are included in the diagram $\mathcal{D}_N$, it remains to show that it is also the case for the set of points contained between them. Let $A(x_A, y_A) \in \{(x,y) \mid x > P(R_N) \text{ and } x/2 + \sqrt{\pi} < y < f_N(x)\}$. Step 4 shows that for any choice of δ and δ' in $[d(R_N), \delta_0 + 1]$, the curves γ_δ and $\gamma_{\delta'}$ are homotopic, and the homotopy is $H : (\sigma, t) \in [0,1] \times [0,3) \longmapsto \gamma_{(1-\sigma)\delta + \sigma\delta'}$. In particular, let us chose $\delta = d(R_N)$ and $\delta' = x_A^2 d(R_N)$. The index of A with respect to $\gamma_\delta = \{(P(R_N), P(R_N)/2 + \sqrt{\pi})\}$ is equal to 0. Meanwhile, by the inequality (20), we have that A is in the interior of the curve $\gamma_{\delta'}$, which means that its index with respect to $\gamma_{\delta'}$ is non-zero. Thus, it must follow that there exists $(\bar{\sigma}, \bar{t}) \in [0,1] \times [0,3)$ such that $A = H(\bar{\sigma}, \bar{t}) \in \mathcal{D}_N$.

Finally, we get the equality

$$\mathcal{D}_N = \left\{ (x,y) \mid x \geq P(R_N) \text{ and } \frac{1}{2}x + \sqrt{\pi} \leq y \leq \frac{x + \sqrt{x^2 + 4(\pi - N \tan \frac{\pi}{N})}}{2} \right\}.$$

3.5.3 If $N \geq 5$ is odd

By the inequalities (5) and (7), we have

$$\mathcal{D}_N \subset \left\{ (x,y) \mid x \geq P(R_N) \text{ and } x/2 + \sqrt{\pi} \leq y \leq f_N(x) \right\},$$

where

$$f_N : x \longmapsto \frac{x + \sqrt{x^2 + 4(\pi - N \tan \frac{\pi}{N})}}{2}. \tag{22}$$

Let us study the lower and upper boundaries of the diagram $\mathcal{D}_N$.

The lower boundary of the diagram $\mathcal{D}_N$:

Since $N - 1$ is even, we have by Section 3.5.2

$$\{(x, x/2 + \sqrt{\pi}) \mid x \geq P(R_{N-1})\} \subset \mathcal{D}_{N-1} \subset \mathcal{D}_N.$$

It remains to prove that

$$\{(x, x/2 + \sqrt{\pi}) \mid x \in [P(R(N), P(R_{N-1})]\} \subset \mathcal{D}_N.$$

To do so, we continuously move two consecutive sides of the polygon R_N so as to align them while keeping the polygon circumscribed. This gives us a continuous (with respect to the Hausdorff distance) family $(W_t)_{t \in [0,1]}$ of convex circumscribed polygons such that $W_0 := R_N$ and W_1 is an element of $\mathcal{P}_{N-1}$, see Figure 8.

Since the family of convex polygons $(W_t)_{t \in [0,1]}$ and the functionals perimeter, area and Cheeger constant are continuous with respect to the Hausdorff distance and $\frac{P(W_1)}{\sqrt{|W_1|}} \geq P(R_{N-1})$ (because of the polygonal isoperimetric inequality in $\mathcal{P}_{N-1}$), we have by the Intermediate Value Theorem

$$\{(x, x/2 + \sqrt{\pi}) \mid x \in [P(R_N), P(R_{N-1})]\} \subset \left\{ \left(\frac{P(W_t)}{\sqrt{|W_t|}}, \sqrt{|W_t|} h(W_t) \right) \;\middle|\; t \in [0,1] \right\} \subset \mathcal{D}_N.$$

We finally have

$$\{(x, x/2 + \sqrt{\pi}) \mid x \in [P(R(N), +\infty)\} \subset \mathcal{D}_N.$$

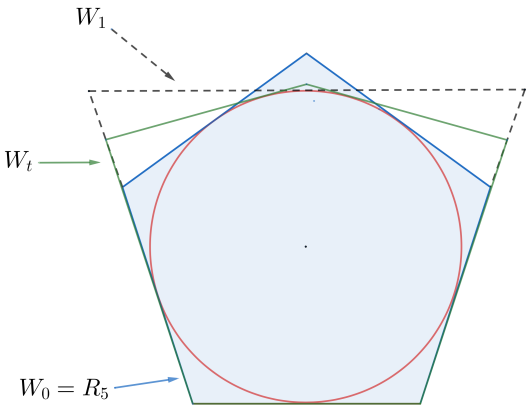

Figure 8: Construction of the circumscribed polygons W_t.

The upper boundary of $\mathcal{D}_N$:

Let us now study the upper boundary of $\mathcal{D}_N$. We recall that the function g_N is defined as follows:

$$\begin{array}{rccl} g_N: & [P(R_N), +\infty) & \longrightarrow & \mathbb{R} \\ & p & \longmapsto & \sup\{h(\Omega) \mid \Omega \in \mathcal{P}_N, \ \ |\Omega| = 1 \text{ and } P(\Omega) = p\}. \end{array} \tag{23}$$

First, let us prove that the problem $\sup\{h(\Omega) \mid \Omega \in \mathcal{P}_N, \ \ |\Omega| = 1 \text{ and } P(\Omega) = p\}$ admits a solution, that we denote by $\Omega_p \in \mathcal{P}_N$.

Take $(\Omega_p^n)_{n\in\mathbb{N}}$ a sequence of elements of $\mathcal{P}_N$ such that $|\Omega_p^n| = 1$ and $P(\Omega_p^n) = p$ for every $n \in \mathbb{N}$, which satisfies

$$\lim_{n\to+\infty} h(\Omega_p^n) = \sup\{h(\Omega) \mid \Omega \in \mathcal{P}_N, \ \ |\Omega| = 1 \text{ and } P(\Omega) = p\}.$$

Since the diameters of the sets (Ω_p^n) are all bounded by p and the involved functionals are invariant by translations, we may assume without loss of generality that there exist a fixed ball $D \subset \mathbb{R}^2$ that contains all the polygons Ω_p^n.

Let $n \in \mathbb{N}$. Since $\Omega_p^n \in \mathcal{P}_N$, the polygon Ω_p^n is the convex hull of N points A_1^n, A_2^n,..., A_N^n. The sequences $(A_1^n), \dots, (A_N^n)$ are bounded in $\mathbb{R}^2$. Thus, by Bolzano-Weirstrass Theorem, there exist $\sigma : \mathbb{N} \longrightarrow \mathbb{N}$ strictly increasing and $A_1, \dots, A_N \in \mathbb{R}^2$ such that $\lim\limits_{n\to+\infty} A_k^{\sigma(n)} = A_k$. By elementary arguments of convex geometry one shows that the convex hull of the points $A_1, \dots, A_N$ defines a convex polygon Ω_p which is also the limit of $(\Omega_p^{\sigma(n)})_n$ with respect to the Hausdorff distance (we refer to [36, Section 1.8] for results on the Hausdorff metric). By the continuity of the perimeter, the area and the Cheeger constant with respect to the Hausdorff distance among convex sets (see [32, Proposition 3.1] for the continuity of the Cheeger constant), we have

$$\begin{cases} |\Omega_p| = \lim\limits_{n\to+\infty} |\Omega_p^{\sigma(n)}| = 1, \\ P(\Omega_p) = \lim\limits_{n\to+\infty} P\big(\Omega_p^{\sigma(n)}\big) = p, \\ h(\Omega_p) = \lim\limits_{n\to+\infty} h\big(\Omega_p^{\sigma(n)}\big) = \sup\{h(\Omega) \mid \Omega \in \mathcal{P}_N, \ \ |\Omega| = 1 \text{ and } P(\Omega) = p\}. \end{cases}$$

Finally, we conclude that $\Omega_p \in \mathcal{P}_N$ is a solution of the problem $\sup\{h(\Omega) \mid \Omega \in \mathcal{P}_N, \ \ |\Omega| = 1 \text{ and } P(\Omega) = p\}$.

Now, let us prove the properties of the function g_N stated in Theorem 5.

1) The function g_N is continuous

Let $p_0 \in [P(R_N), +\infty)$.

- We first show the **superior limit inequality**. Let $(p_n)_{n\geq 1}$ be a real sequence converging to p_0 such that

$$\limsup_{p\to p_0} h(\Omega_p) = \lim_{n\to+\infty} h(\Omega_{p_n}).$$

  As the perimeters of $(\Omega_{p_n})_{n\in\mathbb{N}^*}$ are uniformly bounded, one may assume that the domains $(\Omega_{p_n})_{n\in\mathbb{N}^*}$ are included in a fixed ball. Then by similar arguments as above, the sequence (Ω_{p_n}) converges with respect to the

Hausdorff distance up to a subsequence (that we also denote by p_n for sake of simplicity) to a convex polygon $\Omega^* \in \mathcal{P}_N$.

Again, by the continuity of the perimeter, the area and the Cheeger constant with respect to the Hausdorff distance among convex sets (see [32, Proposition 3.1] for the continuity of the Cheeger constant), we have:

$$\begin{cases} |\Omega^*| = \lim\limits_{n\to+\infty} |\Omega_{p_n}| = 1, \\ P(\Omega^*) = \lim\limits_{n\to+\infty} P(\Omega_{p_n}) = \lim\limits_{n\to+\infty} p_n = p_0, \\ h(\Omega^*) = \lim\limits_{n\to+\infty} h(\Omega_{p_n}) = \limsup\limits_{p\to p_0} h(\Omega_p). \end{cases}$$

Then by the definition of g_N (since $\Omega^* \in \mathcal{P}_N$, $|\Omega^*| = 1$ and $P(\Omega^*) = p_0$), we obtain

$$g_N(p_0) \geq h(\Omega^*) = \lim_{n\to+\infty} h(\Omega_{p_n}) = \limsup_{p\to p_0} h(\Omega_p) = \limsup_{p\to p_0} g_N(p).$$

- It remains to prove **the inferior limit inequality**. Let $(p_n)_{n\geq 1}$ be a real sequence converging to p_0 such that

$$\liminf_{p\to p_0} g_N(p) = \lim_{n\to+\infty} g_N(p_n).$$

By using parallel chord movements (see the proof of Lemma 18), we can construct a sequence of unit area polygons $(K_n)_{n\geq 1}$ with at most N sides, converging to Ω_{p_0} with respect to the Hausdorff distance such that $P(K_n) = p_n$ for sufficiently high values of $n \in \mathbb{N}^*$. By using the definition of g_N, one has

$$\forall n \in \mathbb{N}^*, \quad g_N(p_n) \geq h(K_n).$$

Passing to the limit, we get

$$\liminf_{p\to p_0} g_N(p) = \lim_{n\to+\infty} g_N(p_n) \geq \lim_{n\to+\infty} h(K_n) = h(\Omega_{p_0}) = g_N(p_0).$$

We finally get that $\lim\limits_{p\to p_0} g_N(p) = g_N(p_0)$, so g_N is continuous on $[P(R_N), +\infty)$.

2) The function g_N is strictly increasing

Let us assume by contradiction that g_N is not strictly increasing. Then, there exist $p_2 > p_1 \geq P(R_N)$ such that $g_N(p_2) \leq g_N(p_1)$, and from the equality case in the polygonal isoperimetric inequality, we necessarily have $p_1 > P(R_N)$. Since g is continuous, it reaches its maximum on $[P(R_N), p_2]$ at a point $p^* \in (P(R_N), p_2)$, that is to say

$$\forall \Omega \in \mathcal{P}_N \text{ such that } |\Omega| = 1 \text{ and } P(\Omega) \in [P(R_N), p_2], \quad h(\Omega_{p^*}) = g_N(p^*) \geq h(\Omega). \tag{24}$$

We note that $g_N(p^*) > p^*/2 + \sqrt{\pi}$. Indeed, if it is not the case (i.e., $g_N(p^*) = p^*/2 + \sqrt{\pi}$), we have for sufficiently small $t > 0$

$$g_N(p^* + t) \geq (p^* + t)/2 + \sqrt{\pi} > p^*/2 + \sqrt{\pi} = g_N(p^*),$$

which contradicts the fact that g_N admits a local maximum at p^*.

The assertion (24) shows that Ω_{p^*} is a local maximizer of the Cheeger constant between convex N-gons of unit area. On the other hand, the fact that $h(\Omega_{p^*}) = g_N(p^*) > \frac{P(\Omega_{p^*}) + \sqrt{4\pi}}{2}$ implies that Ω_{p^*} is not a circumscribed polygon (otherwise, it should satisfy the equality (16)). Let us now show that any non-circumscribed polygon Ω (i.e., $T(\Omega) < \frac{P(\Omega)^2}{4|\Omega|}$) can be locally perturbed (while preserving the number of sides) in such a way to increase $|\Omega|^{1/2} h(\Omega)$.

We denote by $(\ell_i)_{i\in[\![1,N]\!]}$ the lengths of the sides of the polygon Ω and $(\alpha_i)_{i\in[\![1,N]\!]}$ its interior angles and take

$$r_0 := \min_{1\leq i\leq N} \frac{\ell_i}{\tan\left(\frac{\pi}{2} - \frac{\alpha_i}{2}\right) + \tan\left(\frac{\pi}{2} - \frac{\alpha_{i-1}}{2}\right)},$$

where we define $\alpha_0 := \alpha_N$. For every $i \in [\![1, N]\!]$ and $\varepsilon \in \mathbb{R}$ such that $|\varepsilon|$ is sufficiently small, we introduce the polygon Ω^i_ε obtained by performing a parallel displacement of the i-th side with the algebraic distance ε, see Figure 9.

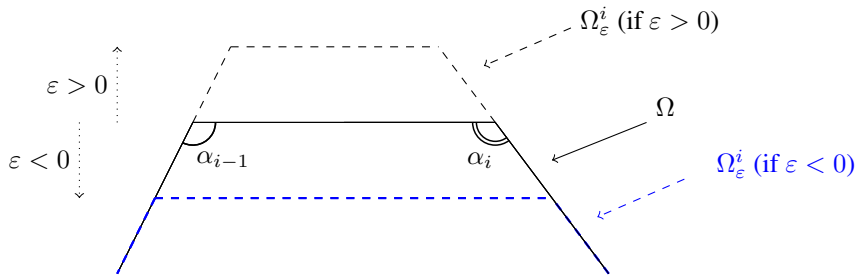

Figure 9: Parallel displacement of the i-th side.

Let us distinguish two cases:

- if $|\Omega| - r_0 P(\Omega) + r_0^2(T(\Omega) - \pi) \geq 0$ (where T is defined in (8)), this means by [26, Theorem 3] that there exists $i \in [\![1, N]\!]$ such that the i-th side of Ω that does not touch the boundary of the Cheeger set C_Ω or touch it in one point. For $\varepsilon > 0$ sufficiently small, the polygons Ω and Ω_ε^i have the same Cheeger set. Thus, we have $|\Omega_\varepsilon^i|^{1/2} h(\Omega_\varepsilon^i) > |\Omega|^{1/2} h(\Omega)$.
- On the other hand if $|\Omega| - r_0 P(\Omega) + r_0^2(T(\Omega) - \pi) < 0$ (where T is defined in (8)), then by [26, Theorem 3], the polygons $(\Omega_\varepsilon^i)_{i \in [\![1,N]\!]}$ (for $|\varepsilon|$ sufficiently small) are Cheeger-regular and thus we have explicit formulas for their Cheeger constants. We write

$$|\Omega_\varepsilon^i|^{1/2} h(\Omega_\varepsilon^i) = \frac{P(\Omega_\varepsilon^i) + \sqrt{P(\Omega_\varepsilon^i)^2 - 4(T(\Omega_\varepsilon^i) - \pi)|\Omega_\varepsilon^i|}}{\sqrt{|\Omega_\varepsilon^i|}} = \frac{P(\Omega_\varepsilon^i)}{\sqrt{|\Omega_\varepsilon^i|}} + \sqrt{\frac{P(\Omega_\varepsilon^i)^2}{|\Omega_\varepsilon^i|} - 4(T(\Omega) - \pi)}, \quad (25)$$

where we used $T(\Omega) = T(\Omega_\varepsilon^i)$ for the last equality.

As stated in the proof of [11, Lemma 23], through elementary geometric arguments, we have for every $i \in [\![1, N]\!]$,

$$\begin{cases} P(\Omega_\varepsilon^i) &= P(\Omega) + \left(\frac{1}{\tan\alpha_{i-1}} + \frac{1}{\tan\alpha_i} + \frac{1}{\sin\alpha_{i-1}} + \frac{1}{\sin\alpha_i}\right)\varepsilon, \\ |\Omega_\varepsilon^i| &= |\Omega| + \ell_i\varepsilon + \frac{1}{2}\left(\frac{1}{\tan\alpha_{i-1}} + \frac{1}{\tan\alpha_i}\right)\varepsilon^2. \end{cases}$$

Thus,

$$\begin{aligned} \frac{P(\Omega_\varepsilon)^2}{|\Omega_\varepsilon|} &= \frac{\left(P(\Omega) + \left(\frac{1}{\tan\alpha_{i-1}} + \frac{1}{\tan\alpha_i} + \frac{1}{\sin\alpha_{i-1}} + \frac{1}{\sin\alpha_i}\right)\varepsilon\right)^2}{|\Omega| + \ell_i\varepsilon + \frac{1}{2}\left(\frac{1}{\tan\alpha_{i-1}} + \frac{1}{\tan\alpha_i}\right)\varepsilon^2} \\ &= \frac{P(\Omega)^2}{|\Omega|} + P(\Omega)\cdot\Psi_i\cdot\varepsilon + \underset{\varepsilon\to 0}{o}(\varepsilon), \end{aligned}$$

where

$$\Psi_i := 2\left(\frac{1}{\tan\alpha_{i-1}} + \frac{1}{\tan\alpha_i} + \frac{1}{\sin\alpha_{i-1}} + \frac{1}{\sin\alpha_i}\right) - \frac{P(\Omega)}{|\Omega|}\ell_i.$$

Let us show that there exists $i \in [\![1, N]\!]$ such that $\Psi_i \neq 0$. We assume by contradiction that $\Psi_i = 0$ for every $i \in [\![1, N]\!]$, we then have

$$\sum_{i=1}^N \Psi_i = 0,$$

which is equivalent to

$$P(\Omega) = \frac{4|\Omega|}{P(\Omega)}\sum_{i=1}^N\left(\frac{1}{\tan\alpha_i} + \frac{1}{\sin\alpha_i}\right) = \frac{4|\Omega|}{P(\Omega)}\sum_{i=1}^N\frac{1}{\tan\frac{\alpha_i}{2}} = \frac{4|\Omega|}{P(\Omega)}\cdot T(\Omega),$$

where $T(\Omega)$ is defined in (8). As stated in Theorem 6, this equality holds if and only if Ω is a circumscribed polygon, which is not the case as assumed above. Thus, there exists $i \in [\![1, N]\!]$ such that $\Psi_i \neq 0$. Then, by performing a parallel displacement (in the suitable sense: $\varepsilon > 0$ if $\psi_i > 0$ and $\varepsilon < 0$ if $\psi_i < 0$) of the ith side, one is able to strictly increase $\frac{P(\Omega)}{|\Omega|^{1/2}}$ and thus, by (25), increase $|\Omega|^{1/2} h(\Omega)$.

3) Comparison between g_N and f_N and asymptotic

- It is immediate by the inclusion $\mathcal{P}_{N-1} \subset \mathcal{P}_N$, the equality $f_{N-1} = g_{N-1}$ (because $N-1$ is even) and the inequality (7) that $f_{N-1} \le g_N \le f_N$ on $[P(R_N), +\infty)$ (we recall that f_N is defined in (22)).
- If we perform a parallel displacement of one of the sides of the regular polygon R_N, we see that there exists $\varepsilon_0 > 0$ and a continuous family (with respect to the Hausdorff distance) of Cheeger-regular polygons $(\Omega_\varepsilon)_{\varepsilon\in[0,\varepsilon_0)}$ with the same interior angles as R_N such that $\frac{P(\Omega_\varepsilon)}{|\Omega_\varepsilon|^{1/2}} > \frac{P(\Omega)}{|\Omega|^{1/2}}$, for every $\varepsilon \in (0, \varepsilon_0)$. This shows that there exists $b_N \ge \frac{P(\Omega_{\varepsilon_0})}{|\Omega_{\varepsilon_0}|^{1/2}} > P(R_N)$ such that

$$\forall x \in [P(R_N), b_N], \quad g_N(x) = \frac{x + \sqrt{x^2 + 4(\pi - N\tan\frac{\pi}{N})}}{2} = f_N(x).$$

- Let us now prove that if Ω is a polygon of N sides and unit area and whose angles are all equal (to $\beta_N := \frac{(N-2)\pi}{N}$), one has

$$P(\Omega) \le 2N\sqrt{\tan\frac{\beta_N}{2}}. \tag{26}$$

We assume that the polygon Ω is included in the half-plane $\{y \ge 0\}$ and that its longest side is given by the segment $[OA]$, where $A(\ell, 0)$ and $\ell > 0$. Since N is odd and all the angles of Ω are equal, we deduce that there exists a unique vertex $B(x_B, \eta)$ which is strictly higher (i.e., has the largest ordinate) than all the other vertices. We can assume without loss of generality that $x_B \ge \ell/2$. We denote by $C(x_C, 0)$ the point of intersection of the line obtained by extending the left side of extremity B and the x-axis and by $D(x_B, 0)$ the orthogonal projection of the point B on the x-axis, see Figure 10. By the convexity of Ω, we have $0 < \theta \le \frac{\beta_N}{2} < \frac{\pi}{2}$, where θ is the angle between the vectors $\overrightarrow{BO}$ and $\overrightarrow{BD}$.

We note that $x_C \le 0$. Indeed,

$$x_C = x_B - (x_B - x_C) = x_B - CD = x_B - \eta\tan\frac{\beta_N}{2} \le x_B - \eta\tan\theta = x_B - OD = 0. \tag{27}$$

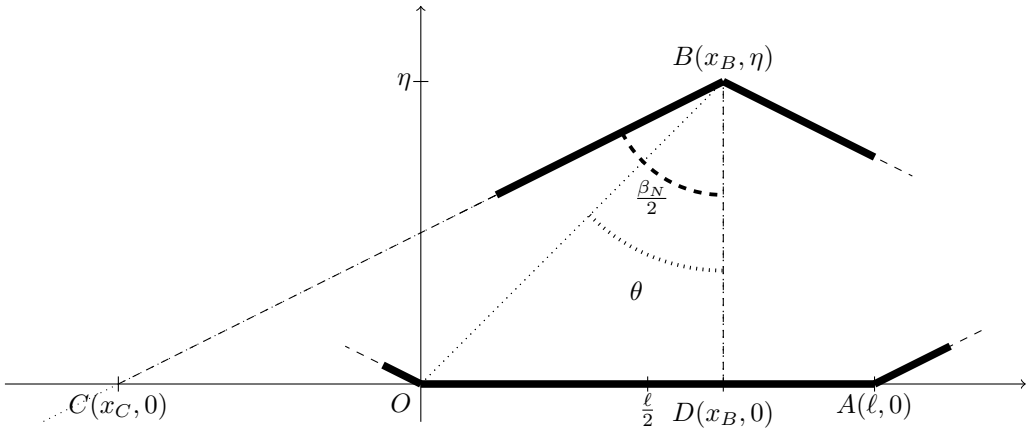

Figure 10: An N-gon with all interior angles equal to β_N.

We have

$$\frac{1}{\tan\frac{\beta_N}{2}} = \operatorname{cotan}\frac{\beta_N}{2} = \frac{\eta}{x_B - x_C} = 2\frac{\frac{1}{2}\ell\eta}{\ell(x_B - x_C)} = 2\frac{\mathcal{S}_{OAB}}{\ell(x_B - x_C)} \le \frac{4}{\ell^2},$$

where $\mathcal{S}_{OAB}$ corresponds to the area of the triangle OAB. The last inequality is a consequence of $\mathcal{S}_{OAB} \le 1$ (because $OAB \subset \Omega$ and $|\Omega| = 1$) and $x_B - x_C \ge x_B \ge \ell/2$ (we recall that $x_C \le 0$ as shown in (27)).

Thus, we have the result

$$P(\Omega) \le N\ell \le 2N\sqrt{\tan\frac{\beta_N}{2}}.$$

This proves that there is no polygon of unit area, N sides and perimeter larger than $2N\sqrt{\tan\frac{\beta_N}{2}}$ whose interior angles are all equal (to β_N). Thus, for every $\Omega \in \mathcal{P}_N$ such that $|\Omega| = 1$ and $P(\Omega) > 2N\sqrt{\tan\frac{\beta_N}{2}}$, we have

$$h(\Omega) \le \frac{P(\Omega) + \sqrt{P(\Omega)^2 - 4\big(T(\Omega) - \pi\big)|\Omega|}}{2|\Omega|} < \frac{P(\Omega) + \sqrt{P(\Omega)^2 + 4\big(\pi - N\tan\frac{\pi}{N}\big)|\Omega|}}{2|\Omega|},$$

where the first inequality corresponds to the inequality (7) and the second (strict) one is a consequence of the inequality $T(\Omega) > N \tan \frac{\pi}{N}$ of Theorem 6 (see (8) for the definition of $T(\Omega)$).

We finally have that

$$\forall x > 2N\sqrt{\tan \frac{\beta_N}{2}}, \qquad g_N(x) < \frac{x + \sqrt{x^2 + 4(\pi - N \tan \frac{\pi}{N})}}{2}.$$

- Since $N \geq 4$, we have

$$\forall x \geq P(R_{N-1}), \qquad \frac{x + \sqrt{x^2 + 4(\pi - (N-1) \tan \frac{\pi}{N-1})}}{2} \leq g_N(x) \leq \frac{x + \sqrt{x^2 + 4(\pi - N \tan \frac{\pi}{N})}}{2}.$$

Thus,

$$g_N(x) \underset{x \to +\infty}{\sim} x.$$

4 Numerical simulations

Since it is not easy to give an explicit description of the upper boundary of the diagram $\mathcal{D}_N$ when N is odd, we perform some simulations in order to have an approximation of the function g_N (defined in Definition 4). We numerically solve the following problems:

$$\max \{h(\Omega) \mid \Omega \in \mathcal{P}_N, \ \ |\Omega| = 1 \text{ and } P(\Omega) = p_0\}, \tag{28}$$

where $p_0 \in [P(R_N), +\infty)$.

4.1 Parametrization of the domains

We parametrize a polygon Ω via its vertices' coordinates $A_1 := (x_1, y_1), \ldots, A_N := (x_N, y_N)$.

- Let us first express the constraint of convexity in terms of the coordinates of the vertices of Ω. It is classical that a polygon Ω is convex if and only if all the interior angles are less than or equal to π. By using the cross product (see [3] for example), the convexity is equivalent to the constraints

$$C_k(x_1, \ldots, x_N, y_1, \ldots, y_N) := (x_{k-1} - x_k)(y_{k+1} - y_k) - (y_{k-1} - y_k)(x_{k+1} - x_k) \leq 0,$$

for $k \in [\![1, N]\!]$, where we used the conventions $A_0 = A_N$ and $A_{N+1} = A_1$.

- The area and the perimeter of Ω are given by the following formulas

$$\begin{cases} f(x_1, \ldots, x_N, y_1, \ldots, y_N) \ := \ P(\Omega) \ = \sum_{k=1}^N \sqrt{(x_{k+1} - x_k)^2 + (y_{k+1} - y_k)^2}, \\ g(x_1, \ldots, x_N, y_1, \ldots, y_N) \ := \ |\Omega| \ = \ \frac{1}{2} \left| \sum_{k=1}^N (x_k y_{k+1} - x_{k+1} y_k) \right| \end{cases}$$

- Finally, we introduce the function

$$\phi : (x_1, \ldots, x_N, y_1, \ldots, y_N) \longmapsto \begin{cases} h(\Omega), & \text{if the polygon } \Omega \text{ does not have overlapping sides,} \\ -1, & \text{if the polygon } \Omega \text{ has overlapping sides,} \end{cases}$$

where Ω is the polygon of vertices $A_1(x_1, y_1), \ldots, A_N(x_N, y_N)$. The Cheeger constant is computed by using an open source Matlab code of B. Bogosel [5]. The algorithm combines the well known result of Kawohl and Lachand-Robert [26] (stated in Theorem 10) which characterizes the Cheeger sets for convex domains and the toolbox Clipper, a very good implementation of polygons' inner parallel sets [5] computation by A. Johnson.

We are now able to write the problem (28) in the following form

$$\begin{cases} \sup\limits_{(x_1, \ldots, y_N) \in \mathbb{R}^{2N}} \phi(x_1, \ldots, y_N), \\ \forall k \in [\![1, N]\!], \quad C_k(x_1, \ldots, x_N, y_1, \ldots, y_N) \leq 0, \\ f(x_1, \ldots, x_N, y_1, \ldots, y_N) = p_0 \\ g(x_1, \ldots, x_N, y_1, \ldots, y_N) = 1. \end{cases}$$

[5] We refer to Definition 9 for the notion of inner parallel sets.

4.2 Computation of the gradients

We want to use Matlab's routine `fmincon` to solve the last problem. To do so, we should compute the gradients of the constraints C_k,f,g and the objective function ϕ.

Since C_k, f and g are explicitly expressed via usual functions of $(x_1, \dots, y_N)$, we obtain explicit formulas for the gradients by straightforward computations. This is not the case for the objective function ϕ, for which we use a shape derivation result proved in [33]. Since Ω is convex, it admits a unique Cheeger set C_Ω that is $C^{1,1}$ (see [1]). We are then in position to use the following result of [33, Corollary 1.2]:

$$h'(\Omega, V) := \lim_{t \to 0} \frac{h(\Omega_t) - h(\Omega)}{t} = \frac{1}{|C_\Omega|} \int_{\partial C_\Omega \cap \partial\Omega} \big(\kappa - h(\Omega)\big) \langle V, n \rangle d\mathcal{H}^1,$$

where $V \in \mathbb{R}^2 \longrightarrow \mathbb{R}^2$ is a smooth perturbation, $\Omega_t := (Id + tV)(\Omega)$ (where $Id : x \longmapsto x$ is the identity map), $n(x)$ is the normal to $\partial\Omega$ at the point x and $\kappa(x)$ is the curvature of $\partial\Omega$ at the point x.

Since Ω is a convex polygon and C_Ω is $C^{1,1}$, the contact set $\Omega \cap C_\Omega$ is given by a finite union of segments. We then have $\kappa = 0$ on $\partial C_\Omega \cap \partial\Omega$. Thus, if we denote by V_{x_k} and V_{y_k} the perturbations respectively associated to the variables x_k and y_k, where $k \in [\![1, N]\!]$, we have

$$\begin{cases} \frac{\partial \phi}{\partial x_k}(x_1, \dots, x_N, y_1, \dots, y_N) &= -\frac{h(\Omega)}{|C_\Omega|} \int_{\partial C_\Omega \cap \partial\Omega} \langle V_{x_k}, n \rangle d\mathcal{H}^1, \\ \frac{\partial \phi}{\partial y_k}(x_1, \dots, x_N, y_1, \dots, y_N) &= -\frac{h(\Omega)}{|C_\Omega|} \int_{\partial C_\Omega \cap \partial\Omega} \langle V_{y_k}, n \rangle d\mathcal{H}^1. \end{cases}$$

4.3 Results

In Figure 11, we plot the points corresponding to 10^5 random convex pentagons and the points corresponding to the optimal pentagons obtained for $p_0 \in \{P(R_5) + 0.02 \cdot k \mid k \in [\![0, 20]\!]\}$, in addition to the graphs of the functions $x \longmapsto x$ and $x \longmapsto f_5(x) := \frac{x + \sqrt{x^2 + 4(\pi - 5\tan\frac{\pi}{5})}}{2}$ whose hypographs represent the inequalities (3) and (7) in the Blaschke–Santaló diagram. The random polygons are generated by using the algorithm presented in [34] (based on a work of P. Valtr, see [38, Section 4]). The Cheeger constants are computed by a Matlab algorithm implemented by B. Bogosel, see [5].

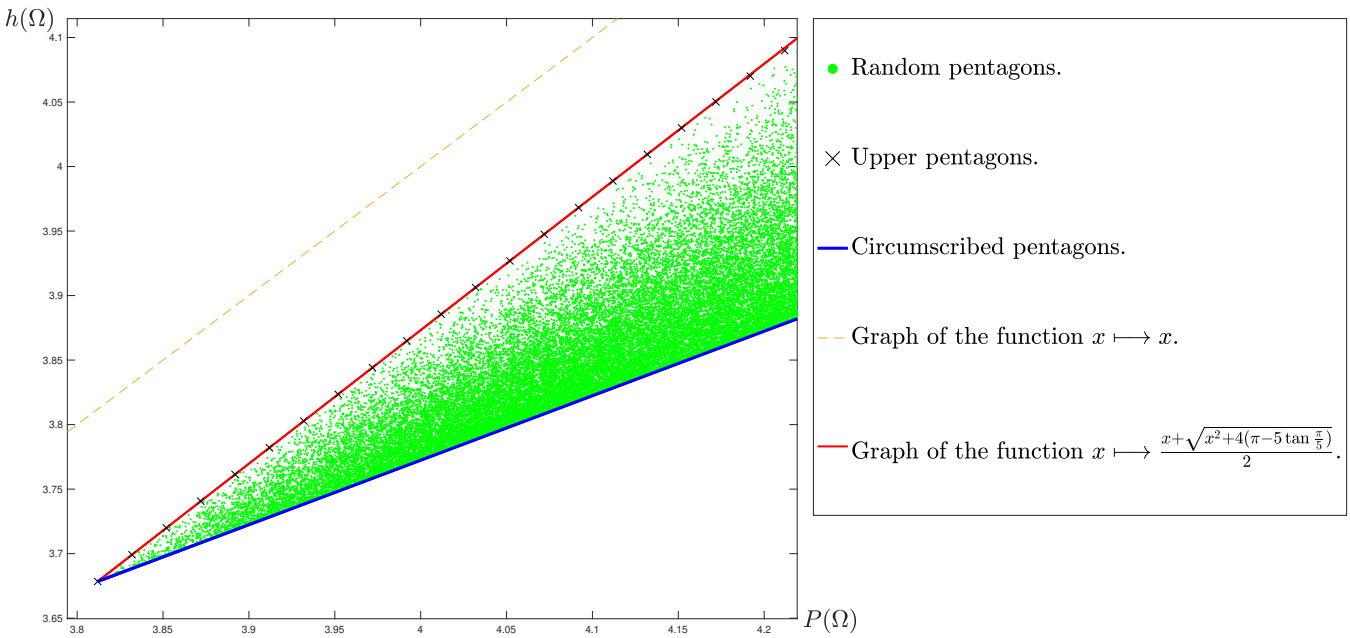

Figure 11: Numerical approximation of the Blaschke–Santaló diagram of convex pentagons.

In Figure 12, we provide a zoom on the upper boundary of the diagram $\mathcal{D}_5$. We observe that the points $(p, g_5(p))_{p \geq P(R_5)}$ (where g_5 is introduced in Definition 4) are at first exactly located on the red and continuous curve corresponding to the graph of the function $x \longmapsto f_5(x) := \frac{x + \sqrt{x^2 + 4(\pi - 5\tan\frac{\pi}{5})}}{2}$, then they detach and become strictly lower than it. We also note that the abscissa c_5 introduced in the statement of Theorem 5 is indeed (as shown in (26)) bounded from above by $10\sqrt{\tan\frac{3\pi}{10}} \approx 11.73$.

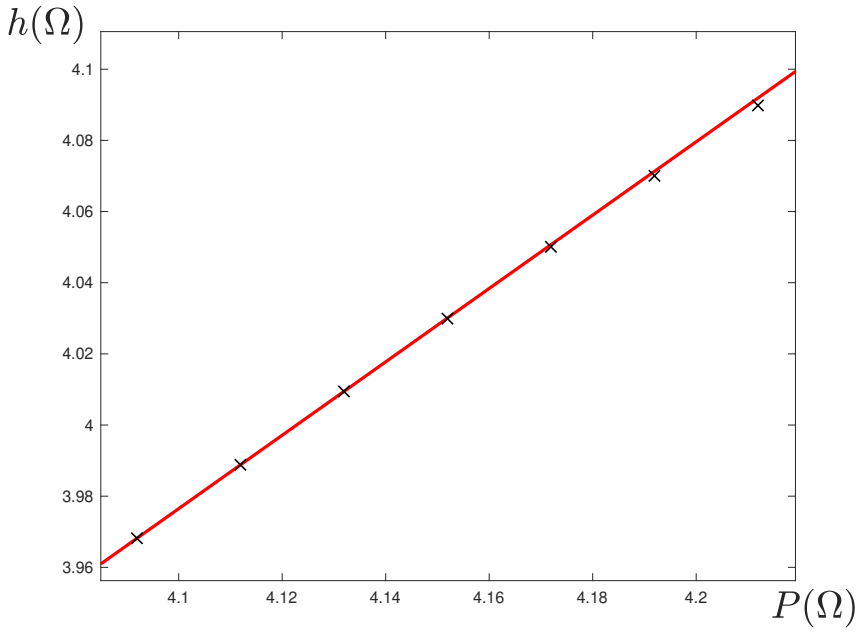

Figure 12: A zoom on the upper boundary of the diagram $\mathcal{D}_5$.

Finally, in Figure 13, we give the obtained optimal pentagons (solutions of (28)) for $p_0 \in \{3.86, 4, 5\}$. We note that for larger values of p_0, the maximizers seem not to be Cheeger-regular.

Values of p_0	3.86	4	5
Optimal pentagons	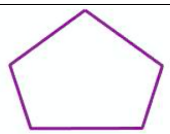		

Figure 13: Numerically obtained (upper) extremal pentagons corresponding to different values of p_0.

Remark 21. *Our numerical approach has been tested on problems for which the solutions are theoretically provided in the present paper (see Theorem 5 and its proof in Section 5). Namely, problems of the type*

$$\min\{h(\Omega) \mid P(\Omega) = p_0,\ |\Omega| = 1 \text{ and } \Omega \in \mathcal{P}_N\} = \frac{p_0}{2} + \sqrt{\pi},$$

where $N \geq 3$ and $p_0 \geq P(R_N)$ and

$$\max\{h(\Omega) \mid P(\Omega) = p_0,\ |\Omega| = 1 \text{ and } \Omega \in \mathcal{P}_N\} = f_N(p_0) = \frac{p_0 + \sqrt{p_0^2 + 4(\pi - N\tan\frac{\pi}{N})}}{2},$$

where N is even.

5 Some applications

In this last section, we give two applications of the results of the present paper.

5.1 Improvement of a classical lower bound for the Cheeger constant of polygons

One early result in the spirit of the inequality (5) is due to R. Brooks and P. Waksman [10], see Proposition 22 below. It gives a lower estimate of the Cheeger constant of convex polygons, which we show to be a consequence of the inequality (5).

Proposition 22. *[10, Theorem 3.] If Ω is a convex polygon, we denote by Ω^* the (unique up to rigid motions) circumscribed polygon which has the same area as Ω and whose angles are the same as those of Ω, then*

$$h(\Omega) \geq h(\Omega^*) = \frac{\sqrt{T(\Omega)} + \sqrt{\pi}}{\sqrt{|\Omega|}}, \tag{29}$$

where the functional T is defined in (8).

Proof. We use the inequality (5) to provide an alternative proof:

$$h(\Omega) \geq \frac{P(\Omega) + \sqrt{4\pi|\Omega|}}{2|\Omega|} \geq \frac{2\sqrt{|\Omega|}\sqrt{T(\Omega)} + \sqrt{4\pi|\Omega|}}{2|\Omega|} = \frac{\sqrt{T(\Omega)} + \sqrt{\pi}}{\sqrt{|\Omega|}} = \frac{\sqrt{T(\Omega^*)} + \sqrt{\pi}}{\sqrt{|\Omega^*|}},$$

where we respectively used (5) and (9) for the first and second inequalities and the fact that Ω^* has the same area and interior angles as Ω for the last equality.

□

5.2 On the stability of the Cheeger constant of polygons

We use the inequality (5) and [12, Proposition 2.1] to give a quantitative version of the polygonal Faber-Krahn type inequality for convex polygons (see [11]).

Proposition 23. *Take $N \geq 3$. There exists a positive constant C_N such that for every convex N-gon Ω with unit area, there exists a rigid motion ρ of $\mathbb{R}^2$ such that*

$$h(\Omega)^2 - h(R_N)^2 \geq C_N d^H\big(\Omega, \rho(R_N)\big)^2, \tag{30}$$

where R_N is a regular polygon of unit area and N sides.

Proof. Take $N \geq 3$ and Ω a convex N-gon. We have by the inequality (5) applied to Ω and the equality (16) applied to the circumscribed polygon R_N

$$P(\Omega) \leq 2(h(\Omega) - \sqrt{\pi}) \quad \text{and} \quad P(R_N) = 2(h(R_N) - \sqrt{\pi}).$$

Thus,

$$\begin{aligned} P(\Omega)^2 - P(R_N)^2 &\leq 4(h(\Omega) - \sqrt{\pi})^2 - 4(h(R_N) - \sqrt{\pi})^2 \\ &= 4\big(h(\Omega)^2 - h(R_N)^2 - 2\sqrt{\pi}\big(h(\Omega) - h(R_N)\big)\big) \\ &\leq 4\big(h(\Omega)^2 - h(R_N)^2\big), \end{aligned}$$

where the last inequality is a consequence of the polygonal Faber-Krahn type inequality $h(\Omega) \geq h(R_N)$, see [11].

On the other hand, it is proved in [12, Proposition 2.1] that there exists $C_N > 0$ depending only on N such that

$$P(\Omega)^2 - P(R_N)^2 \geq 4C_N d^H\big(\Omega, \rho(R_N)\big)^2.$$

Finally, by combining the latter inequalities, we get the announced result. □

Remark 24. *The quantitative inequality* (30) *shows in particular the stability of the Cheeger constant in the neighborhood of regular polygons among convex polygons with the same number of sides and the same area. In the sense that if the Cheeger constants of a convex polygon and a regular polygon with the same number of sides and the same area are close, then the polygon looks (up to rigid motions) like the regular one. A similar result can be obtained for non convex N-gons, see [13].*

Acknowledgments

The author would like to warmly thank the anonymous referee for his careful reading and detailed report that considerably helped to improve the presentation of the material of the paper. The author would also like to thank Dorin Bucur and Jimmy Lamboley for stimulating conversations and valuable comments.

This work was partially supported by the project ANR-18-CE40-0013 SHAPO financed by the French Agence Nationale de la Recherche (ANR) and by the Alexander von Humboldt Foundation.

References

[1] F. Alter and V. Caselles. Uniqueness of the Cheeger set of a convex body. *Nonlinear Anal.*, 70(1):32–44, 2009.

[2] T. M. Apostol and M. A. Mnatsakanian. Figures circumscribing circles. *Amer. Math. Monthly*, 111(10):853–863, 2004.

[3] S. Bartels and G. Wachsmuth. Numerical approximation of optimal convex shapes. *SIAM J. Sci. Comput.*, 42(2):A1226–A1244, 2020.

[4] W. Blaschke. Konvexe Bereiche gegebener konstanter Breite und kleinsten Inhalts. *Math. Ann.*, 76(4):504–513, 1915.

[5] B. Bogosel. Matlab codes for the computation of the Cheeger constant of planar convex sets; 15.06.2017 [accessed 02.11.2021]. `https://github.com/bbogo/Cheeger_patch`.

[6] A. Boulkhemair. On a shape derivative formula in the Brunn-Minkowski theory. *SIAM J. Control Optim.*, 55(1):156–171, 2017.

[7] L. Brasco. On principal frequencies and inradius in convex sets. *Bruno Pini Math. Anal. Semin.*, page 20, 2018.

[8] L. Brasco. On principal frequencies and isoperimetric ratios in convex sets. *Ann. Fac. Sci. Toulouse Math.*, page 25, 2019.

[9] L. Briani, G. Buttazzo, and F. Prinari. Some inequalities involving perimeter and torsional rigidity. *Appl. Math. Optim.*, 84(3):2727–2741, 2021.

[10] R. Brooks and P. Waksman. The first eigenvalue of a scalene triangle. *Proc. Amer. Math. Soc.*, 100(1):175–182, 1987.

[11] D. Bucur and I. Fragalà. A Faber-Krahn inequality for the Cheeger constant of N-gons. *J. Geom. Anal.*, 26(1):88–117, 2016.

[12] M. Caroccia and F. Maggi. A sharp quantitative version of Hales' isoperimetric honeycomb Theorem. *J. Math. Pures Appl. (9)*, 106(5):935–956, 2016.

[13] M. Caroccia and R. Neumayer. A note on the stability of the Cheeger constant of N-gons. *J. Convex Anal.*, 22(4):1207–1213, 2015.

[14] J. Cheeger. A lower bound for the smallest eigenvalue of the Laplacian. In *Problems in analysis (Papers dedicated to Salomon Bochner, 1969)*, pages 195–199. 1970.

[15] S. J. Cox and M. Ross. Extremal eigenvalue problems for starlike planar domains. *J. Differential Equations*, 120(1):174–197, 1995.

[16] G. Crasta, I. Fragalà, and F. Gazzola. A sharp upper bound for the torsional rigidity of rods by means of web functions. *Arch. Ration. Mech. Anal.*, 164(3):189–211, 2002.

[17] A. Delyon, A. Henrot, and Y. Privat. Nondispersal and density properties of infinite packings. *SIAM J. Control Optim.*, 57(2):1467–1492, 2019.

[18] A. Delyon, A. Henrot, and Y. Privat. The missing (A, d, r) diagram. *Ann. de l'inst. Fourier (to appear)*, 2021.

[19] A. Figalli, F. Maggi, and A. Pratelli. A note on Cheeger sets. *Proc. Amer. Math. Soc.*, 137(6):2057–2062, 2009.

[20] I. Ftouhi. On the Cheeger inequality for convex sets. *J. Math. Anal. Appl.*, 504(2):Paper No. 125443, 26, 2021.

[21] I. Ftouhi and J. Lamboley. Blaschke–Santaló diagram for volume, perimeter, and first Dirichlet eigenvalue. *SIAM J. Math. Anal.*, 53(2):1670–1710, 2021.

[22] A. Henrot and M. Pierre. *Shape variation and optimization*, volume 28 of *EMS Tracts in Mathematics*. European Mathematical Society (EMS), Zürich, 2018.

[23] M. A. Hernández Cifre and G. Salinas. Some optimization problems for planar convex figures. Number 70, part I, pages 395–405. 2002. IV International Conference in "Stochastic Geometry, Convex Bodies, Empirical Measures & Applications to Engineering Science", Vol. I (Tropea, 2001).

[24] M. A. Hernández Cifre, G. Salinas, and S. S. Gomis. Complete systems of inequalities. *JIPAM. J. Inequal. Pure Appl. Math.*, 2(1):Article 10, 12, 2001.

[25] V. Julin and G. Saracco. Quantitative lower bounds to the Euclidean and the Gaussian Cheeger constants. *Ann. Fenn. Math.*, 46(2):1071–1087, 2021.

[26] B. Kawohl and T. Lachand-Robert. Characterization of Cheeger sets for convex subsets of the plane. *Pacific J. Math.*, 225(1):103–118, 2006.

[27] G. P. Leonardi, R. Neumayer, and G. Saracco. The Cheeger constant of a Jordan domain without necks. *Calc. Var. Partial Differential Equations*, 56(6):Paper No. 164, 29, 2017.

[28] G. P. Leonardi and A. Pratelli. On the Cheeger sets in strips and non-convex domains. *Calc. Var. Partial Differential Equations*, 55(1):Art. 15, 28, 2016.

[29] G. P. Leonardi and G. Saracco. Minimizers of the prescribed curvature functional in a Jordan domain with no necks. *ESAIM Control Optim. Calc. Var.*, 26:Paper No. 76, 20, 2020.

[30] I. Lucardesi and D. Zucco. On Blaschke–Santaló diagrams for the torsional rigidity and the first Dirichlet eigenvalue. *Annali di Mat. Pura ed Appli. (1923 -)*, 60(2), 2021.

[31] E. Parini. An introduction to the Cheeger problem. *Surv. Math. Appl.*, 6:9–21, 2011.

[32] E. Parini. Reverse Cheeger inequality for planar convex sets. *J. Convex Anal.*, 24(1):107–122, 2017.

[33] E. Parini and N. Saintier. Shape derivative of the Cheeger constant. *ESAIM Control Optim. Calc. Var.*, 21(2):348–358, 2015.

[34] V. Sander. An article on a good algorithm for generating random convex polygons; [accessed 02.11.2021]. `http://cglab.ca/~sander/misc/ConvexGeneration/convex.html`.

[35] L. Santaló. Sobre los sistemas completos de desigualdades entre treselementos de una figura convexa plana. *Math. Notae*, 17:82–104, 1961.

[36] R. Schneider. *Convex Bodies: The Brunn-Minkowski Theory*. Cambridge University Press, 2nd expanded edition edition, 2013.

[37] J. Steiner. Über parallele Flächen. *Monatsber. preuß. Acad. Wiss.*, Vol. 2:114–118, 1882.

[38] P. Valtr. Probability that n random points are in convex position. *Discrete Comput. Geom.*, 13(3-4):637–643, 1995.

[39] M. Van den Berg and G. Buttazzo. On capacity and torsional rigidity. *Bull. Lond. Math. Soc.*, 53(2):347–359, 2021.

[40] M. Van den Berg, G. Buttazzo, and A. Pratelli. On the relations between principal eigenvalue and torsional rigidity. *Commun. Contemp. Math. (to appear)*, 2020.

(Ilias Ftouhi) FRIEDRICH-ALEXANDER-UNIVERSITÄT ERLANGEN-NÜRNBERG, DEPARTMENT OF MATHEMATICS, CHAIR OF APPLIED ANALYSIS (ALEXANDER VON HUMBOLDT PROFESSORSHIP), CAUERSTR. 11, 91058 ERLANGEN, GERMANY.

Email address: **ilias.ftouhi@fau.de**